NASA CONTRACTOR REPORT

NASA CR-1419

INFERENCE OF STRATOSPHERIC TEMPERATURE AND MOISTURE PROFILES FROM OBSERVATIONS OF THE INFRARED HORIZON

by Frederick B. House and George Ohring

Prepared by
GCA CORPORATION
Bedford, Mass.
for Langley Research Center

NATIONAL AERONAUTICS AND SPACE ADMINISTRATION • WASHINGTON, D. C. • AUGUST 1969

INFERENCE OF STRATOSPHERIC TEMPERATURE AND MOISTURE PROFILES FROM OBSERVATIONS OF THE INFRARED HORIZON

By Frederick B. House and George Ohring

Issued by Originator as Report No. GCA-TR-69-5-N

Prepared under Contract No. NAS 1-7572 by
GCA CORPORATION
Bedford, Mass.

for Langley Research Center

NATIONAL AERONAUTICS AND SPACE ADMINISTRATION

For sale by the Clearinghouse for Federal Scientific and Technical Information
Springfield, Virginia 22151 – CFSTI price $3.00

FOREWORD

This report presents results of theoretical research on Atmospheric Inferences from Infrared Horizon Measurements performed under National Aeronautics and Space Administration Contract NAS1-7572 for Langley Research Center.

This study is concerned with the problem of extracting information on atmospheric structure from infrared radiance measurements near the earth's horizon. The study includes an assessment of the 15μ CO_2 band and the H_2O rotational band as potential spectral regions whose radiance measurements can be used to infer temperature and moisture profiles in the stratosphere. Investigations including inversion techniques, absorption band structures, error analyses and problems relating to radiometer design constitute portions of the study.

Gratitude is extended to the scientists at NASA/Langley Research Center for their interest, technical assistance and guidance during the course of the study. These scientists include Mr. R. Davis who is technical monitor of the program and official government representative concerning any questions and availability of the results, and also include Mrs. R. Whitman and Messrs. T. McKee, J. Dodgen and H. Curfman.

ABSTRACT

This study concerns the feasibility of inferring temperature and moisture profiles in the stratosphere from horizon radiances in the 15 micron CO_2 band and the H_2O rotational band. Investigations are performed of inversion techniques, absorption band structures, error analyses and problems related to instrument design. A relatively simple inference method termed the "instant inversion" technique is developed and applied successfully to both theoretical radiance profiles and observed horizon radiances from Project Scanner. A detailed analysis of these inversion results leads to a recommended measurement and data reduction technique to determine both temperature and moisture profiles in the stratosphere and lower mesosphere.

TABLE OF CONTENTS

INFERENCE OF STRATOSPHERIC TEMPERATURE AND MOISTURE PROFILES FROM OBSERVATIONS OF THE INFRARED HORIZON

By Frederick B. House and George Ohring
GCA Corporation, GCA Technology Division
Bedford, Massachusetts

SUMMARY

Infrared radiance emitted by the atmosphere above the earth's hard horizon varies with tangent height depending on the concentration and spectral absorbing properties of the atmospheric gases and on their pressure and temperature distribution with altitude. Therefore, measured horizon radiances contain information about these atmospheric parameters. This study concerns the feasibility of inferring temperature and moisture profiles from horizon radiances in the 15μ CO_2 band and the H_2O rotational band.

Investigations are performed of inversion techniques, absorption band structures, error analyses and problems related to instrument design. A relatively simple method termed the "instant inversion" technique is developed and tested extensively. The successful application of this technique to both theoretical profiles and observed horizon radiances from Project Scanner demonstrates the feasibility of inferring atmospheric parameters. A detailed analysis of these inversion results leads to a recommended measurement and data reduction technique to determine both temperature and moisture profiles in the stratosphere and lower mesosphere. It is concluded that useful temperatures can be obtained in the altitude range from about 10 to 65 km and water vapor mixing ratios can be determined within the 10 to 50 km altitude range.

INTRODUCTION

The inadequacy of present stratospheric measurements of temperature and moisture are apparent when one considers available instrumentation, geographical coverage and observational platforms for in-situ measurements. Temperature profiles are available in the lower stratosphere up to altitudes of 25 to 30 km from standard meteorological balloon soundings. Various rocket-borne instruments have been developed for sounding the atmosphere between 30 to 55 km, with occasional measurements to higher altitudes. Moisture profiles are made infrequently in the stratosphere, and measurements require sophisticated instruments such as frost-point hygrometers. When one considers the frequency and geographical coverage of these measurements on a world-wide basis, the lack of routine observations over oceanic regions and in the Southern Hemisphere is quite pronounced, even in the troposphere.

The need for a better specification of the general state of the atmosphere at any time is indicated by numerical experiments using general circulation models (ref. 1 and 2). Prediction models currently under development require temperature, moisture and wind information up to altitudes of 40 km (ref. 3). The requirement for data in the upper atmosphere will increase as prediction models become more sophisticated.

Possibilities of remotely probing the atmosphere from satellite platforms are attractive in view of the requirement of global coverage of meteorological data. The second generation of meteorological satellites in the NIMBUS series will incorporate sophisticated radiometers for remote probing of the atmosphere in the infrared region of the electromagnetic spectrum. Outgoing radiance signals from atmospheric absorption bands depend on the concentration and spectral absorbing properties of the gases and on the pressure and temperature distribution with altitude. Therefore, radiance measurements contain information about these atmospheric parameters. The inference of parameters from radiance measurements is commonly termed "the inversion problem."

Active absorption bands in the infrared region of the spectrum include carbon dioxide (CO_2), water vapor (H_2O) and ozone (O_3). Assuming CO_2 is uniformly mixed in the atmosphere, it is possible to infer vertical temperature profiles from radiance measurements in the 15μ CO_2 band. With knowledge of the temperature profile, it is then possible to determine vertical concentration profiles of water vapor and ozone based on radiance measurements in the 6.3 or 20 to 40μ bands of H_2O and in the 9.6μ O_3 band, respectively.

Measurements by current nadir-viewing radiometers will allow accurate temperature inferences to altitudes from the surface to about 30 km (ref. 4). Moisture inferences are possible only in the troposphere (ref. 5), and determination of total O_3 concentration and an estimate of its altitude distribution (ref. 6) appear feasible from nadir experiments.

The possibility of inferring atmospheric parameters from horizon radiance measurements has not received the attention given to nadir-viewing experiments. The reason for this probably lies in the fact that temperature and moisture data in the stratosphere are not as useful as data in the troposphere, and that inferences apply to the region of the atmosphere above cloud-top altitudes. It should be pointed out, however, that tropospheric inferences of temperature suffer from the same cloud problem (ref. 7). Inferences of atmospheric parameters from horizon radiances have several important advantages: excellent vertical resolution, enhanced signal due to the long optical paths associated with limb viewing, and no background interference since the radiances are viewed against the cold of space. Data derived from horizon radiances certainly would be a complimentary adjunct to current nadir-viewing experiments.

The current study constitutes a detailed investigation of the temperature and moisture inference problem from observations of the infrared horizon. Work along similar lines has been performed concurrently at the Langley Research Center (ref. 8 and 9), and the possibility of the concept was apparent in an investigation of horizon definition (ref. 10) for spacecraft attitude control. The study includes an assessment of the 15μ CO_2 band and the H_2O rotational band as potential spectral regions whose radiance measurements can be used to infer temperature and moisture profiles in the stratosphere. Investigations of inversion techniques, absorption band structures, error analyses and problems relating to radiometer design constitute parts of the study.

Benefits to be realized from routine measurements of temperature, moisture and ozone profiles in the stratosphere are many. These data would aid research on the nature of stratospheric warmings, troposphere-stratosphere interactions, the 26-month cycle in the equatorial stratospheric winds, diurnal variation at the stratopause (ref. 11), stratospheric general circulation, global distribution of moisture and ozone, radiative balance in the stratosphere and lower mesosphere, circulation of trace constituents and the photochemistry of ozone. Practical applications of these data include operational problems associated with high-flying aircraft like the SST, effect on development of numerical prediction models and problems related to National Defense including atmospheric effects on the operation of offensive and defensive missile systems.

SYMBOLS

A_o	constant in an equation for a straight line (equation 15)
A_1	slope coefficient in an equation for a straight line (equation 15)
B	Planck radiance, watts/m^2-sr-cm^{-1}
$\overline{B}$	effective Planck radiance for a given tangent height, watts/m^2-sr
C_1	constant in Planck formula, 1.1909 x 10^{-8} watts-cm^4/m^2-sr
C_2	constant in Planck formula, 1.4389 cm deg
h	tangent height, km
i	counting index
J	source function, watts/m^2-sr-cm^{-1}
L	generalized absorption coefficient
N	horizon radiance, watts/m^2-sr
n	counting index
P	pressure, mbar
re	random error
rms	root-mean-square error
se	systematic error
T	temperature, ^oK
$\overline{T}$	effective emitting temperature, ^oK
U^*	reduced optical path length of a gas
W	mixing ratio of a gas, g/kg
WF	weighting function, k^{-1}
x	independent variable along a ray path
z	altitude variable, km
z'	altitude of the effective emitting level, km

Δ increment of a variable

ϵ emittance

ν wavenumber, cm^{-1}

ν_c central wavenumber of a bandpass filter, cm^{-1}

ν_1 lower wavenumber of a spectral interval, cm^{-1}

ν_2 upper wavenumber of a spectral interval, cm^{-1}

$$\sum \text{ term} = \sum_{i=1}^{n} \left(\frac{P_i}{P_o}\right)^2 \left(\frac{T_o}{T_i}\right)^{3/2}$$

τ transmittance

Subscripts

a anterior portion of ray path

C carbon dioxide

H water vapor

p posterior portion of ray path

ν at a wavenumber

$\Delta\nu$ specified spectral interval

INSTANT INVERSION TECHNIQUE

Background

A distinction should be made between the concepts of conventional in-situ measurement and remote sensing of atmospheric parameters. In-situ measurements of atmospheric parameters such as temperature, pressure and moisture are usually made by separate instruments which allow a point-by-point determination of each parameter as a function of altitude. The instruments are carried through the atmosphere by some platform such as a balloon, parachute or rocket. The concept of remote atmospheric sensing is quite different in that the vertical profile of radiant energy, emitted by the atmosphere, is the only measured quantity. A single observation of radiance in a given absorption band of an atmospheric gas is related to a conglomeration of many parameters at different altitudes of the atmosphere. The magnitude of a radiance measurement is related principally to temperature, pressure, concentration of absorbing gas and the optical properties of the absorption band. There is indeed a difference between the concepts of in-situ measurement and remote radiometric sensing of atmospheric parameters.

As stated earlier, the objective of this study is the extraction of two interesting parameters, temperature and moisture, from radiance observations of the infrared horizon. In order to determine either of these parameters, it is necessary to have knowledge of all other parameters affecting the observed radiance. For example, to determine temperature it is necessary to have knowledge about pressure, the amount of gas and its optical properties. If the determination is of moisture or the concentration of water vapor, it is necessary to know the distribution of pressure and temperature in the atmosphere as well as water vapor's optical properties. The whole problem is further complicated by the fact that a single radiance observation is an integral of the emitted energy from many levels in the atmosphere.

The spectral regions of interest in this study include the CO_2 band from 615 to 715 cm^{-1} and the H_2O band from 315 to 475 cm^{-1}. Examples of radiance profiles in these bands are presented in figure 1.

The determination of atmospheric parameters from radiance measurements is commonly termed the inversion problem. The discussion of this section presents the theoretical background and justification of a simple method termed the "instant inversion technique." This technique is developed for both temperature and moisture inferences, and it takes advantage of the limb-viewing geometry associated with horizon radiance measurements in the infrared region of the electromagnetic spectrum.

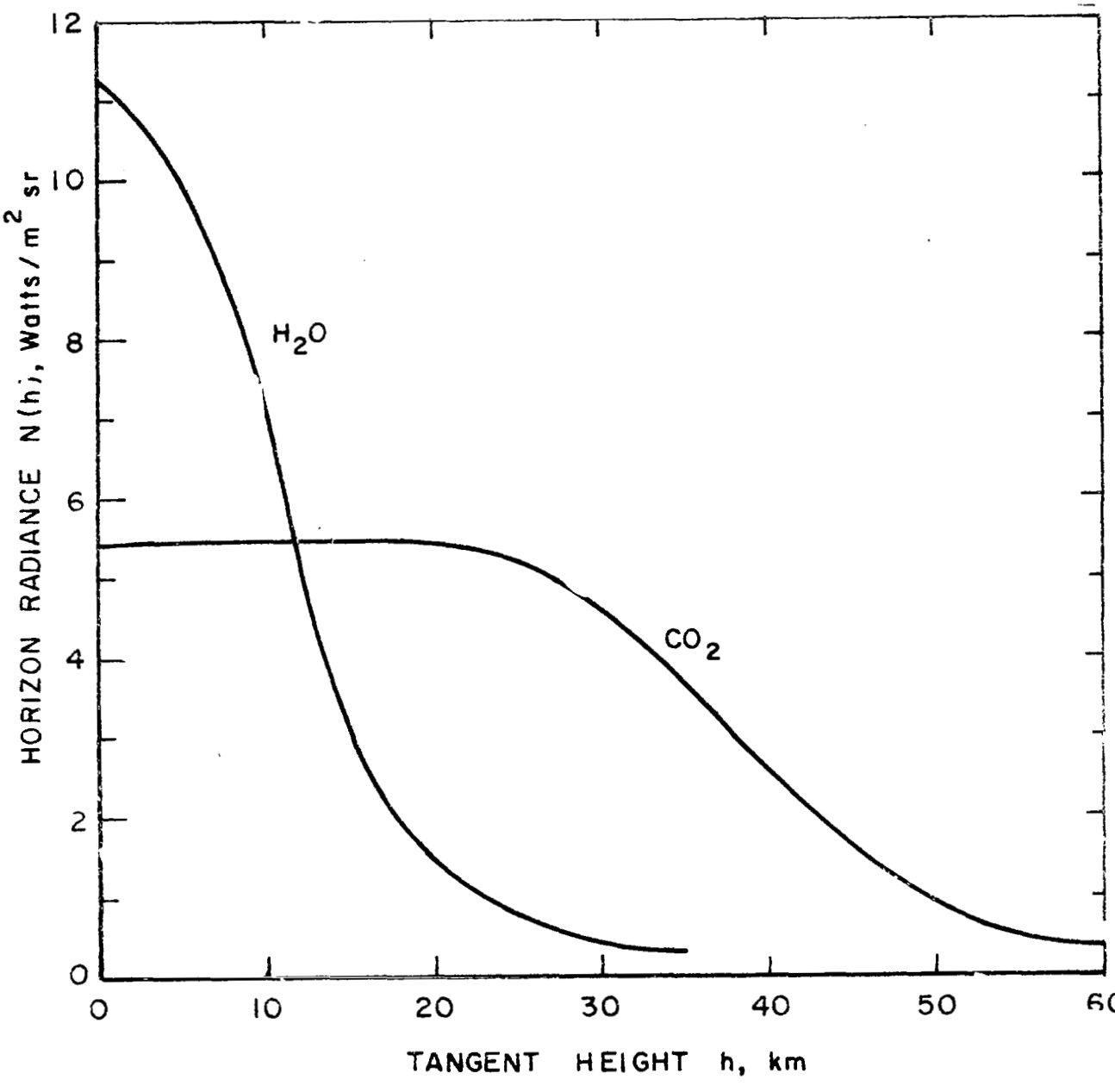

Figure 1. Measured horizon radiance profiles in the CO_2 band (615 to 715 cm^{-1}) and the H_2O band (315 to 475 cm^{-1}) from Project Scanner observations (ref. 8).

Temperature Inversion Theory

The horizon radiance that would be sensed by a satellite-borne radiometer in figure 2 is given by the exact form of the radiative transfer equation

$$N_{\Delta\nu}(h) = -\int_{\nu_1}^{\nu_2} \int_{1}^{\tau_\nu(h,-\infty)} J_\nu[T(x)]\, d\tau_\nu(h,x)\, d\nu \qquad (1)$$

where it is assumed that the atmosphere is the only source of emission and that there are no obstructions such as clouds or the earth's surface. Equation (1) indicates that the horizon radiance is the sum of incremental energy sources at temperature T integrated long the line-of-sight, each having a change in spectral transmittance of $d\tau_\nu$. The measured radiance arising from a given absorption band is integrated over the entire band between limits ν_1 and ν_2. The inversion problem consists in the extraction of temperature information from the integral equation (1).

As long as the assumption of local thermodynamic equilibrium is valid, the source function $J_\nu[T(z)]$ is the Planck function

$$J_\nu[T(z)] = B_\nu[T(z)] = \frac{C_1 \nu^3}{\exp\left(\frac{C_2 \nu}{T}\right) - 1} \qquad (2)$$

Thus, after integration over the band, equation (1) may be expressed by

$$N_{\Delta\nu}(h) = \int_{+\infty}^{-\infty} B_{\Delta\nu}[T(z)]\, \frac{\partial \tau_{\Delta\nu}}{\partial x}\, dx \qquad (3)$$

It is assumed in the instant inversion technique that the Planck radiance $B_{\Delta\nu}$ may be expressed by an average Planck radiance $\bar{B}_{\Delta\nu}[T(z')]$, associated with a single temperature at a specified altitude z'. With this approximation, equation (3) is easily integrated

$$N_{\Delta\nu}(h) = (1 - \tau_{\Delta\nu})\, \bar{B}_{\Delta\nu}[T(z')] = \epsilon_{\Delta\nu}(h)\, \bar{B}_{\Delta\nu}[T(z')] \qquad (4)$$

Solving for the Planck radiance in equation (4) gives

$$\bar{B}_{\Delta\nu}[T(z')] = \frac{N_{\Delta\nu}(h)}{\epsilon_{\Delta\nu}(h)} \qquad (5)$$

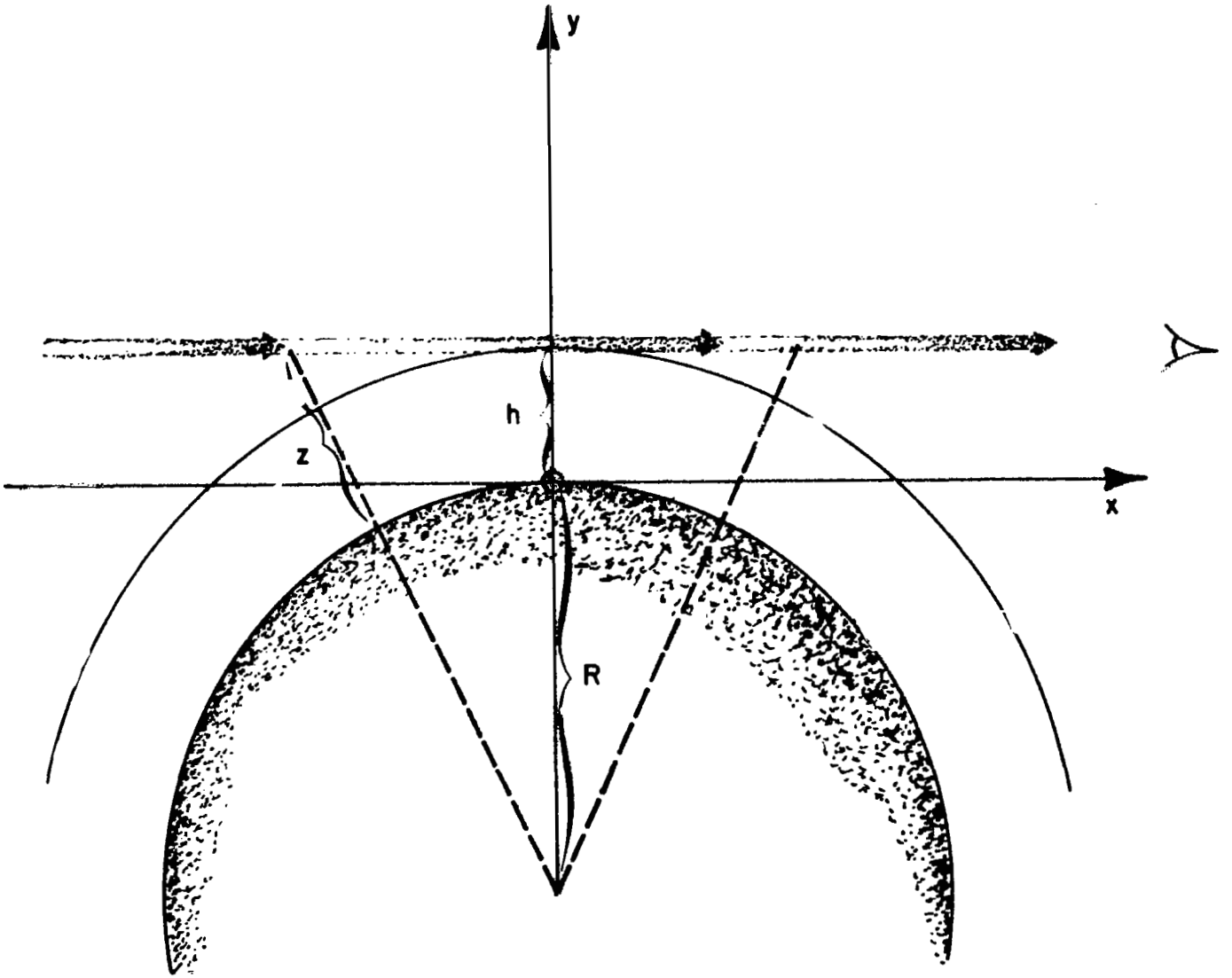

Figure 2. Limb viewing geometry.

which is interpreted in terms of temperature using a form of equation (2) after including the spectral band width.

In this study the coordinate x does not extend from the dimensions $+\infty$ to $-\infty$, but is bounded by a spherical shell at an altitude of 90 km above the earth's surface. The total path length emittance $\epsilon_{\Delta\nu}(h)$ in equation (5) may be expressed as the sum of two integrals representing the contributions by the portions of the atmosphere anterior and posterior to the tangent height point of the ray path.

$$\epsilon_{\Delta\nu}(h) = - \int_{90}^{h} \left(\frac{\partial \tau_{\Delta\nu}}{\partial z} \right)_a dz - \int_{h}^{90} \left(\frac{\partial \tau_{\Delta\nu}}{\partial z} \right)_p dz \qquad (6)$$

The weighting function or change of transmittance along the ray path with respect to the altitude coordinate is of particular interest in depicting the physics of the problem. Assuming spherical symmetry, the summed weighting function WF(h,z) at a given altitude is the sum of anterior and posterior contributions

$$WF(h,z) = \left(\frac{\partial \tau_{\Delta\nu}}{\partial z} \right)_a - \left(\frac{\partial \tau_{\Delta\nu}}{\partial z} \right)_p \qquad (7)$$

Figure 3 illustrates the variation in weighting functions with altitude for different tangent heights. The curves give a good approximation of the contribution by different levels of the atmosphere to the radiance at a given tangent height. As can be seen by the peaked nature of the functions, the radiation for tangent heights above 25 km originates from a rather narrow altitude increment above the reference level. This optical property of the atmosphere is unique to limb-viewing and justifies the basic assumption of the instant inversion technique (equation 5), that the Planck radiance for a representative temperature can be inferred from the ratio of the observed radiance and the total emittance.

Moisture Inversion Theory

The approach to the inference of moisture profiles follows a similar line of thought as that for temperature inferences. However, the total emittance of water vapor is the computed quantity rather than the Planck radiance, and the mixing ratio W_H is one parameter in an exponential expression for the total emittance. The emittance is computed by

$$\epsilon_H(h) = \frac{N_H(h)}{\bar{B}_H[T(z')]} \qquad (8)$$

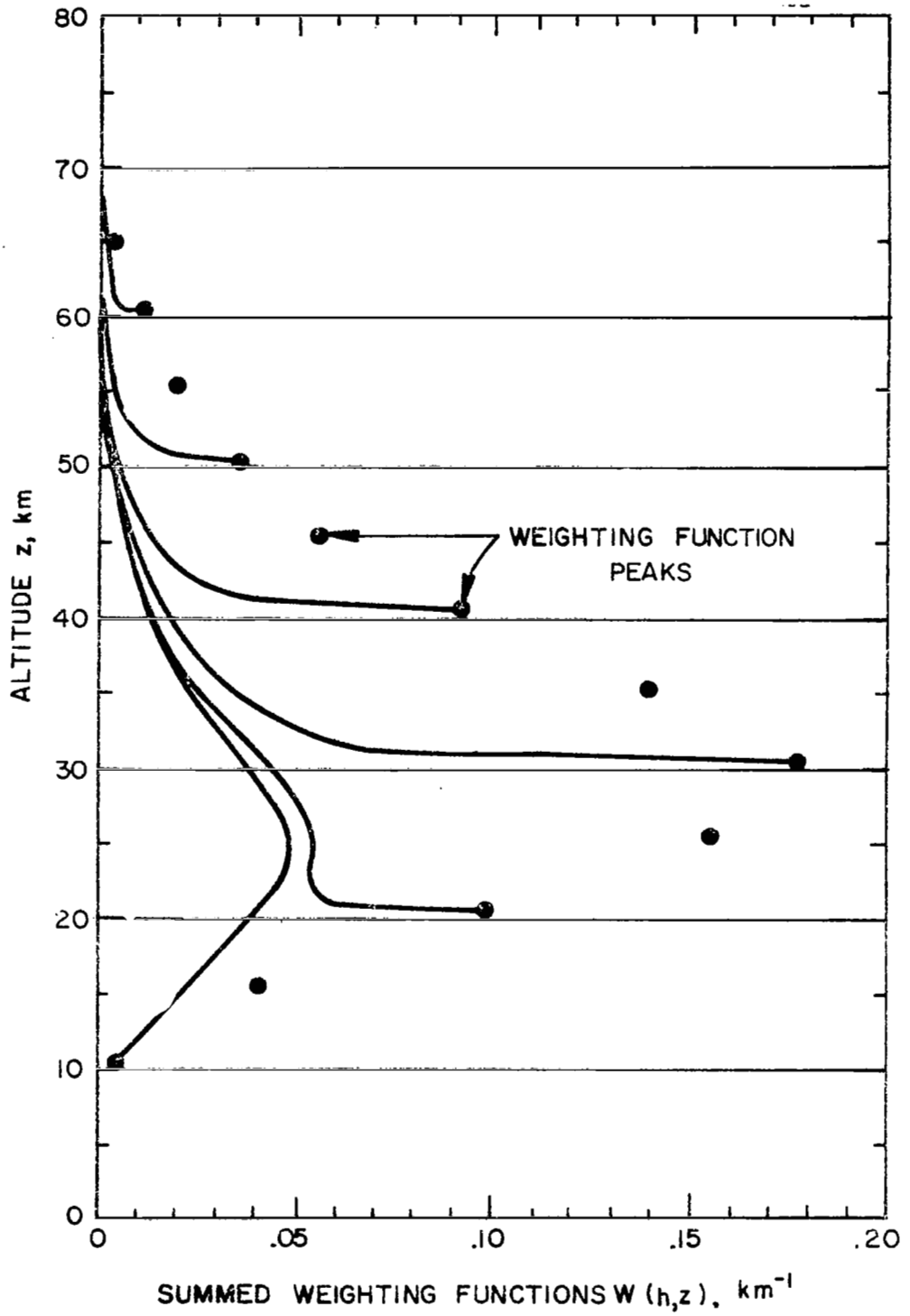

Figure 3. Variation of summed weighting functions (equation 7) for tangent heights at 5-km intervals - ICAO Standard Atmosphere 615 to 715 cm^{-1}. Complete weighting function shown at 10-km intervals.

where the subscript (H) refers to the rotational water vapor band (315 to 475 cm^{-1}) and the Planck radiance is determined from the temperature derived previously from the CO_2 inversion. In a nonscattering atmosphere, the transmittances of H_2O and CO_2 are related to the emittances by

$$\tau_H(h) = 1 - \epsilon_H(h) \tag{9}$$

and

$$\tau_C(h) = 1 - \epsilon_C(h) \tag{10}$$

where the subscript (C) refers to the carbon dioxide band (615 to 715 cm^{-1}).

The problem at hand is to establish the relationships between the two transmittances in (9) and (10) based on transmission theory for the respective absorption bands. A convenient transmission model for this discussion is that developed by Elsasser (ref. 11) where the transmittances are expressed by the sum of common logarithms, Log U^* + Log L. In this case U^* is the reduced optical path length of the gas and L is the generalized absorption coefficient. The path lengths for each gas are defined as

$$U^*_C = \sum_{i=1}^{n} \left(\frac{P_i}{P_o}\right)^2 \left(\frac{T_o}{T_i}\right)^{3/2} W_C \, \Delta x = W_C \sum \tag{11}$$

and

$$U^*_H = 1.292 \times 10^{-3} \sum_{i=1}^{n} \left(\frac{P_i}{P_o}\right)^2 \left(\frac{T_o}{T_i}\right)^{3/2} W_H \, \Delta x = 1.292 \times 10^{-3} W_H \sum \tag{12}$$

where the capital sigma is a shortened notation for the summation term across n shells along the line of sight, and P_o and T_o are standard pressure and temperature, respectively. It is noted that the summation term is the same for both gases when it is assumed that the mixing ratio of water vapor is constant above the tangent height altitude. Units of optical path length are cm for CO_2 and gm/cm^2 (or precipitable cm) for H_2O. Since the total emittance of CO_2 is known, it is possible to evaluate the term $\sum$ in equation (11)

$$\sum = \frac{U^*_C}{W_C} \tag{13}$$

when it is assumed that CO_2 is uniformly mixed in the stratosphere. Substitution of equation (13) in (12) and solving for the mixing ratio gives

$$W_H = \frac{U^*_H W_C}{1.292 \times 10^{-3} U^*_C} \tag{14}$$

Both of the optical path lengths U^*_H and U^*_C are determined from their respective emittances with knowledge of the band-pass filters of the radiometers.

The above technique for inferring moisture profiles will work effectively provided that the H_2O and CO_2 band-pass filters on the radiometer are matched optically. This statement implies that the optical path lengths for both gases are approximately the same as a function of altitude. Putting this condition in another context, this statement implies that the summed weighting functions in figure 3 peak at the same altitudes and that the radiance curves in figure 1 should increase in magnitude at about the same altitudes.

The CO_2 band (615 to 715 cm^{-1}) and the H_2O band (315 to 475 cm^{-1}) measured by Project Scanner radiometers are not optically suited for water vapor inferences using the solution described by equation (14). However, the moisture inference concept may be investigated by utilizing temperature and pressure profiles based on meteorological soundings of the atmosphere at the time of observation. These data allow a direct computation of the U^*_C/W_C term in equation (14) rather than deriving this term from the total emittance parameter of CO_2.

Summary Remarks

In the instant inversion technique the assumption is made that the radiative transfer equation may be approximated by the product of the total path length emittance and the average Planck radiance. There is physical justification for this assumption since the weighting functions for the CO_2 band indicate that the emitted radiant power originates from a rather narrow altitude region above the tangent height level. With this approximation it is possible to determine atmospheric temperature from the ratio of observed radiance to emittance. The technique may then be applied to radiance measurements in the water vapor rotational band to infer moisture profiles once the temperature structure is known providing that the two bands are matched optically.

TECHNIQUE DEVELOPMENT

In this section a number of physical aspects of the inversion problem are considered which relate to the transmittance properties of the atmosphere in the CO_2 and H_2O rotational bands. The total emittance in the instant inversion technique depends on the concentration of gas, the pressure and temperature or density along the ray path and the optical characteristics of each band. The value of emittance at a given level is influenced by the atmospheric structure above the tangent height level. Of course the H_2O emittance varies with the magnitude of water vapor mixing ratio. Consideration is also given in this section to the dispersion characteristics of the horizon radiance with altitude and the effects of the lack of thermodynamic equilibrium.

Altitude Dispersion

The technique of temperature inversion should work quite well for all tangent heights above 20 km because the weighting functions are definitely peaked above this level. Consider the curves of figure 4 which illustrate the same information as is in the weighting functions (figure 3) but in a different manner. The altitude dispersion or percent of total radiance and its relation to the altitude above the tangent height level is shown by the curves. For example, the 50-percent radiance level for a 20-km tangent height is about 10 km (at a z' height at 30 km). In sharp contrast, the 50-percent radiance level for a 60-km tangent height is about 1.3 km. The curves of figure 4 also illustrate the fact that the shape of the weighting functions is constantly changing with altitude. In principle, the physics of the atmosphere are such that the higher the altitude the better the temperature inference using the instant inversion technique.

In all the results compiled in this study, the 50-percent radiance level for each tangent height is assumed to be the effective emitting level (z') for purposes of the instant inversion technique [see equation (5)].

Emittance Calibration

The total emittance in the CO_2 band depends basically on the temperature and pressure structure of the atmosphere. Knowledge of the emittance variation with tangent height for a given radiance profile is essential to the success of the inversion technique [see equation (5)]. An emittance calibration technique was developed as part of this study to account for the variation in emittance with air mass structure. The technique depends on an additional piece of information which is assumed to be characteristic of a particular atmosphere. Two parameters were investigated for this purpose, the height of the 10 mbar surface and the summed radiances between

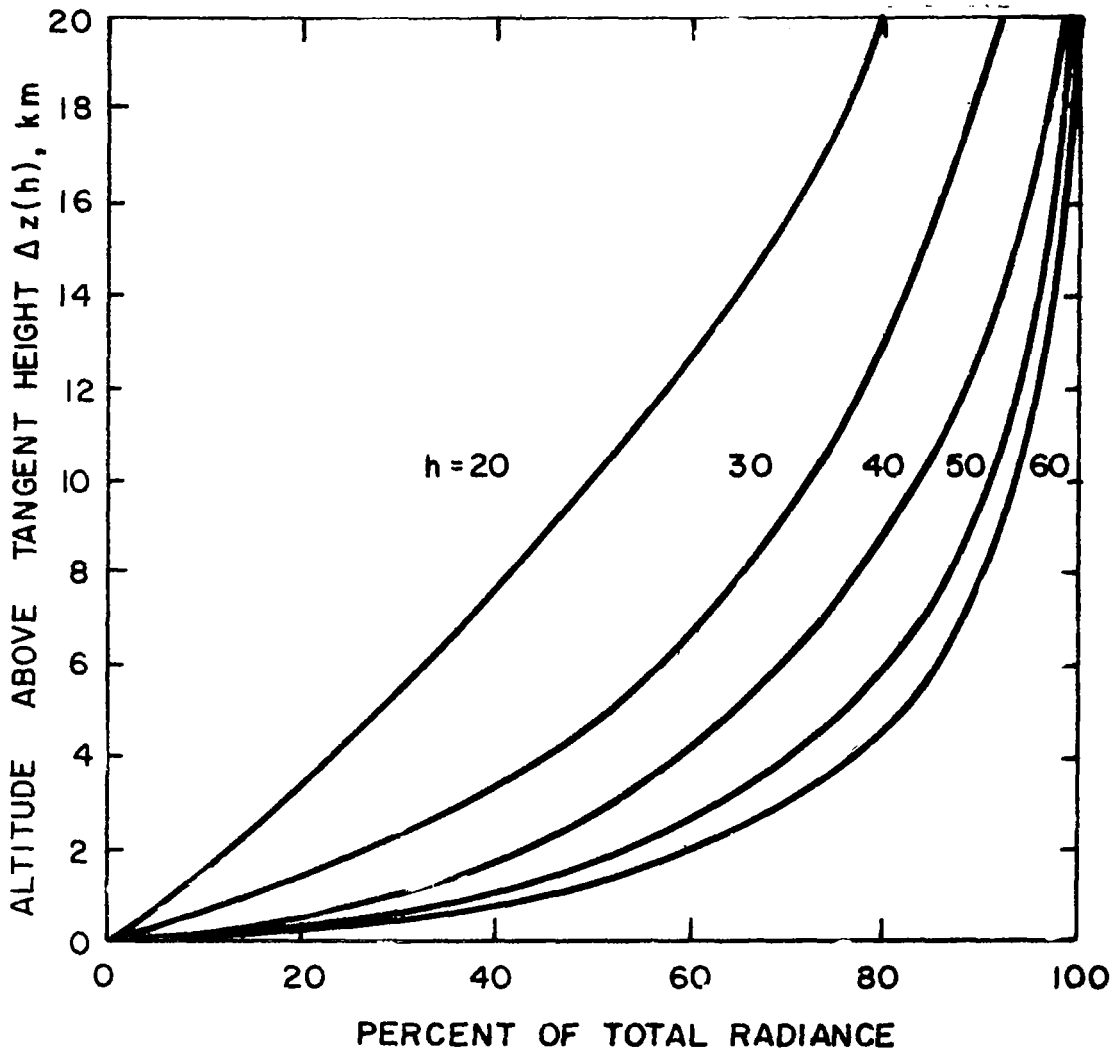

Figure 4. Altitude dispersion of the horizon radiance for different tangent heights – ICAO Standard Atmosphere 615 to 715 cm^{-1}.

tangent heights of 20 to 60 km in steps of 5 km. Linear correlations were developed between the variation in emittance with tangent height for twenty climatological profiles (ref. 10) and the two calibration parameters. Calculations of the emittance for these profiles were performed by the LRC technical monitor, Mr. R. E. Davis.

Figure 5 illustrates the correlation of emittance with the height of the 10-mbar surface for a tangent height of 30 km. The plotted points are computed emittances for each of the 20 climatological profiles. A strong coupling between the emittance and the height of the 10-mbar surface is quite evident in the graph. The correlation between emittances and the 10-mbar surface for tangent heights from 20 to 60 km shows a similar linear coupling. Based on these data it is possible to account for the variation of emittances using an empirical relationship based on a straight line curve fit to the data at each tangent height. Thus, the emittance at a tangent height may be expressed by the equation

$$\epsilon(h) = A_1 \, HT_{\text{10-mbar surface}} + A_o \tag{15}$$

A least squares fit to the data in figure 5 leads to computed constants of $A_1 = 0.051$ km^{-1} and $A_o = -0.930$ when the height of the 10-mbar surface is given in kilometers.

The results of linear curve fits to emittance data for different tangent heights are presented in Tables I and II where the emittance calibration parameters are the height of the 10-mbar surface and the area under the radiance-tangent curve, respectively. Included in the tabulated data are the coefficients for equation (15), the statistical standard error of the estimate and the standard error percentage.

Lack of Thermodynamic Equilibrium

Lack of thermodynamic equilibrium implies that the source function in the radiative transfer equation is different from the Planck function [see equation (2)]. This problem was investigated using the model described in reference 10. Radiance profile calculations were made for the Standard Atmosphere, assuming two conditions; one where the lack of equilibrium conditions existed and the second where the Planck formula was assumed to be valid. The change in the magnitudes of radiances at each tangent height indicates the lack of equilibrium. The results are presented in figure 6 where the ordinate values indicate the decrease in computed radiances due to the lack of thermodynamic equilibrium. The effect is quite small in the altitude range of interest for the instant inversion technique, no more than 1.1 percent for the radiance at a 60-km tangent height. Correction for this effect is accomplished by dividing the observed horizon radiances $N_{\Delta\nu}(h)$ in equation (5) by the ordinate values for each tangent height, represented by the curve in figure 6.

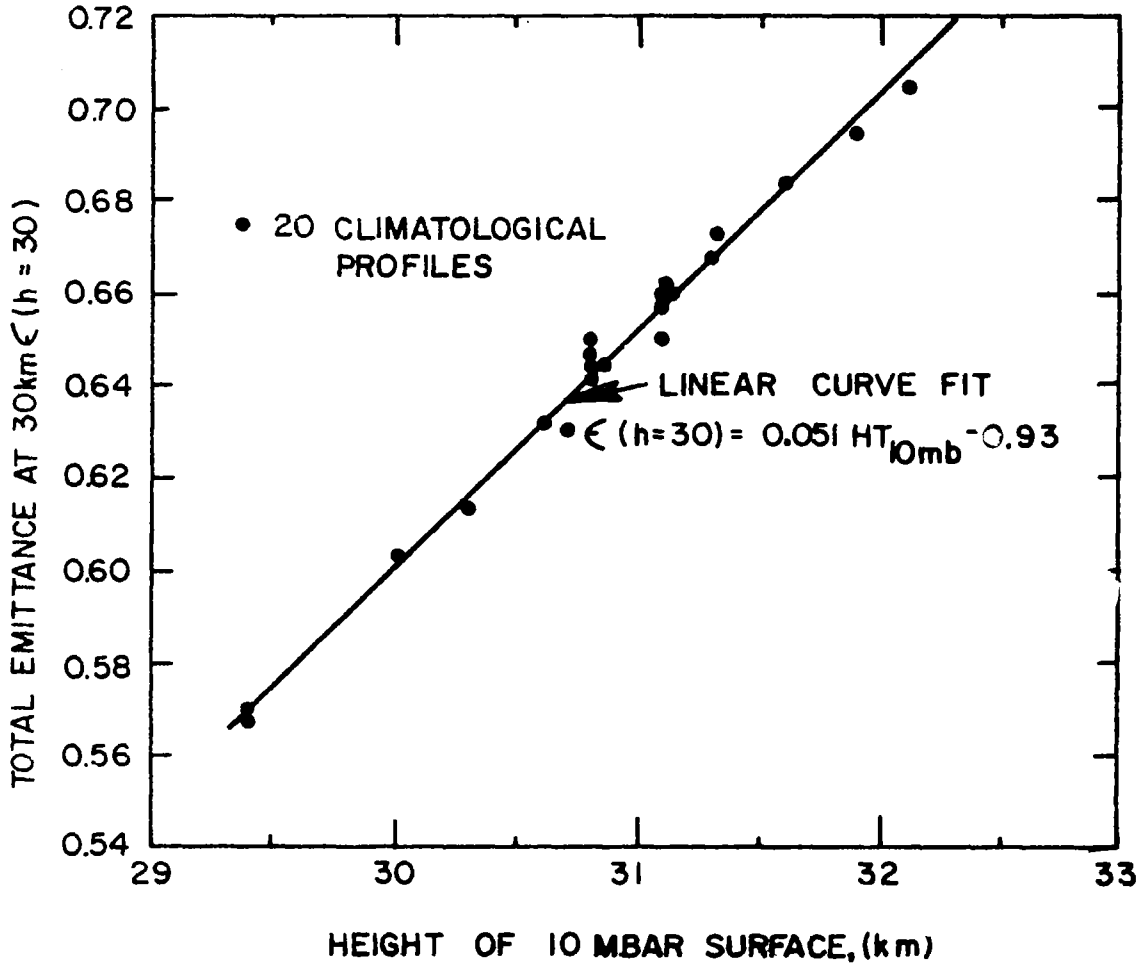

Figure 5. Correlation of total emittances with heights of the 10 mbar surface for a tangent height of 30 km – 615 to 715 cm^{-1}.

TABLE I. — RESULTS OF LINEAR CURVE FITS TO EMITTANCE DATA FOR DIFFERENT TANGENT HEIGHTS

Parameter - 10 mbar Surface

Tangent Height, km	Curve Fit Coefficients Slope, A_1*	Const, A_0	Standard Error of Estimate	Standard Error Percentage
20	1.65-2	4.35-1	2.46-3	0.26
25	3.50-2	-2.52-1	2.43-3	0.29
30	5.10-2	-9.30-1	3.83-3	0.59
35	5.48-2	-1.25	5.36-3	1.21
40	4.80-2	-1.20	5.89-3	2.10
45	3.54-2	-9.27-1	4.93-3	2.92
50	2.30-2	-6.13-1	3.43-3	3.43
55	1.40-2	-3.76-1	2.05-3	3.56
60	7.48-3	-1.99-1	1.15-3	3.56

*Units of km^{-1}

TABLE II. — RESULTS OF LINEAR CURVE FITS TO EMITTANCE DATA FOR DIFFERENT TANGENT HEIGHTS

Parameter - Summed Radiances

Tangent Height, km	Curve Fit Coefficients Slope, A_1*	Const, A_0	Standard Error of Estimate	Standard Error Percentage
20	2.53-3	8.87-1	4.26-3	0.45
25	5.15-3	7.07-1	5.85-3	0.71
30	7.64-3	4.60-1	6.92-3	1.07
35	8.34-3	2.38-1	5.74-3	1.29
40	7.40-3	9.68-2	3.84-3	1.37
45	5.51-3	3.25-2	2.50-3	1.48
50	3.61-3	1.06-2	1.26-3	1.26
55	2.19-3	3.36-3	7.50-4	1.30
60	1.17-3	3.41-3	5.57-4	1.72

*Units of $(watts/m^2\text{-}sr)^{-1}$

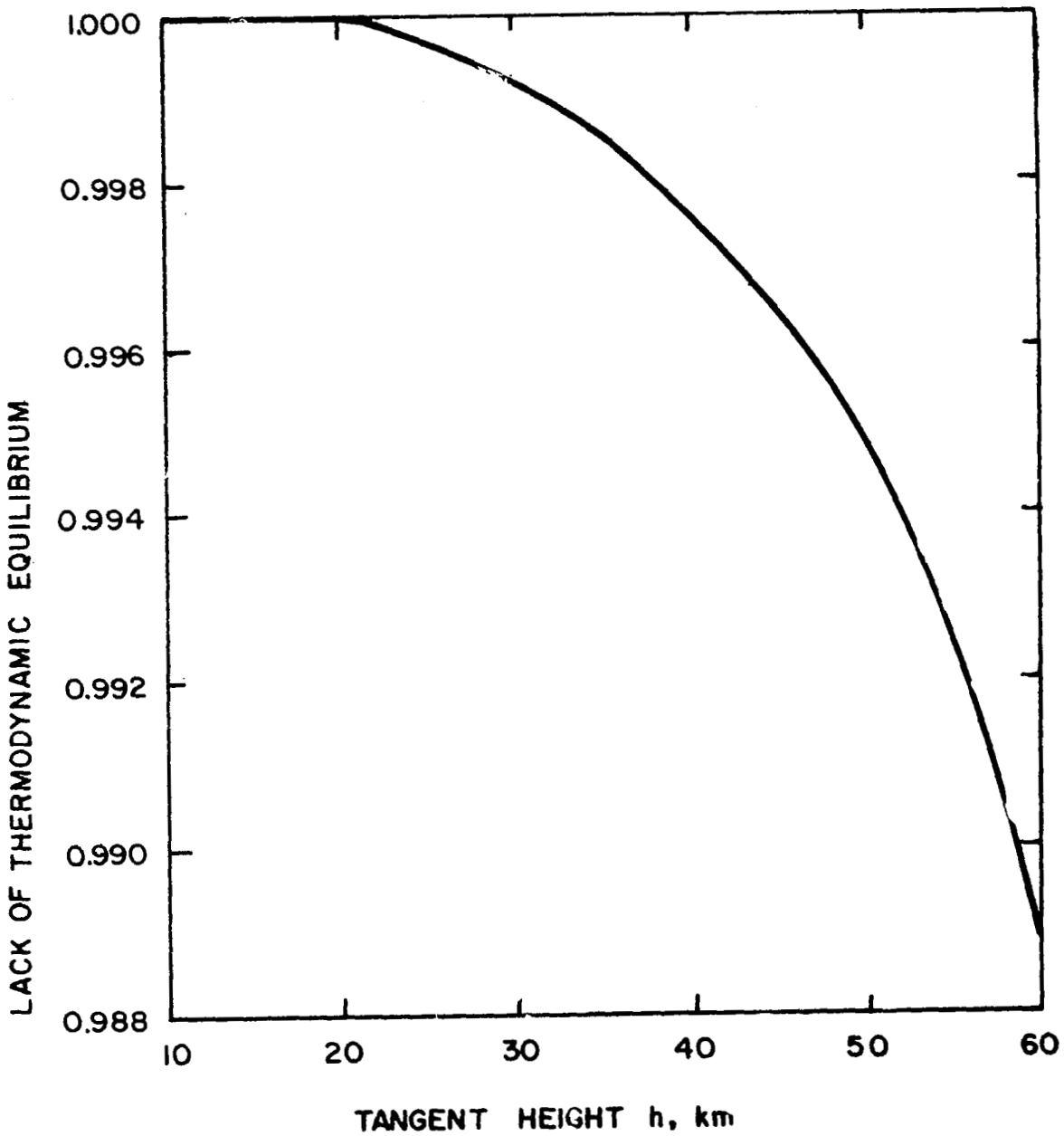

Figure 6. Lack of thermodynamic equilibrium as a function of tangent height - ICAO Standard Atmosphere.

Comparison of CO_2 and H_2O Band Emittances

An analysis was made of the band emittance properties for both CO_2 and H_2O in the spectral regions associated with the Project Scanner observations. The transmission model of Elsasser (ref. 12) is convenient for purposes of this discussion. In this model the transmittances are expressed by the sum of common logarithms, Log U^* + Log L, where U^* is the reduced optical path length and L is a generalized absorption coefficient which varies in magnitude within each band. The band emittances were computed for both CO_2 and H_2O — the results are presented in figure 7 for an effective temperature of 233°K. The band emittances are plotted as a function of $\text{Log}_{10} \sum$ term which is a parameter common to both gases and defined in equations (11) and (12). The family of curves for H_2O illustrate the change in band emittance for different concentrations of water vapor mixing ratios.

In addition to the results in figure 7, computations were completed for a number of different effective temperatures corresponding to those found in the stratosphere. It is possible to determine the sensitivity of band emittance to temperature from these data. Results indicated that the CO_2 band emittance was insensitive to temperature variations; however, the H_2O band emittance exhibited a systematic shift of significant magnitude. The emittance increases with temperature for a given $\text{Log}_{10} \sum$ term in figure 7. An empirical formula was developed for the H_2O band which accounts for this temperature effect.

$$\text{Log}_{10} \sum_{\bar{T}} = \text{Log}_{10} \sum_{T=233^\circ K} + 0.0063(\bar{T} - 233) \qquad (16)$$

The effect of the formula is to shift the family of curves in figure 7 either to the left or right depending on whether the temperature is warmer or colder than 233°K, respectively.

It should be noted that the spectral intervals for CO_2 and H_2O are not matched optically for purposes of inferring mixing ratios from horizon radiances. A comparison of curves in figure 7 will illustrate this point. The rise in the CO_2 band emittance occurs in the Log $\sum$ term range between magnitudes of about 1 and 5, whereas, the rise in the H_2O band emittance occurs at magnitudes between 5 and 8 for reasonable values of mixing ratio in the stratosphere.

In the design of an instrument system for mixing ratio inferences, these two curves should increase in approximately the same range of Log $\sum$ term magnitudes. The implication of these results is plainly

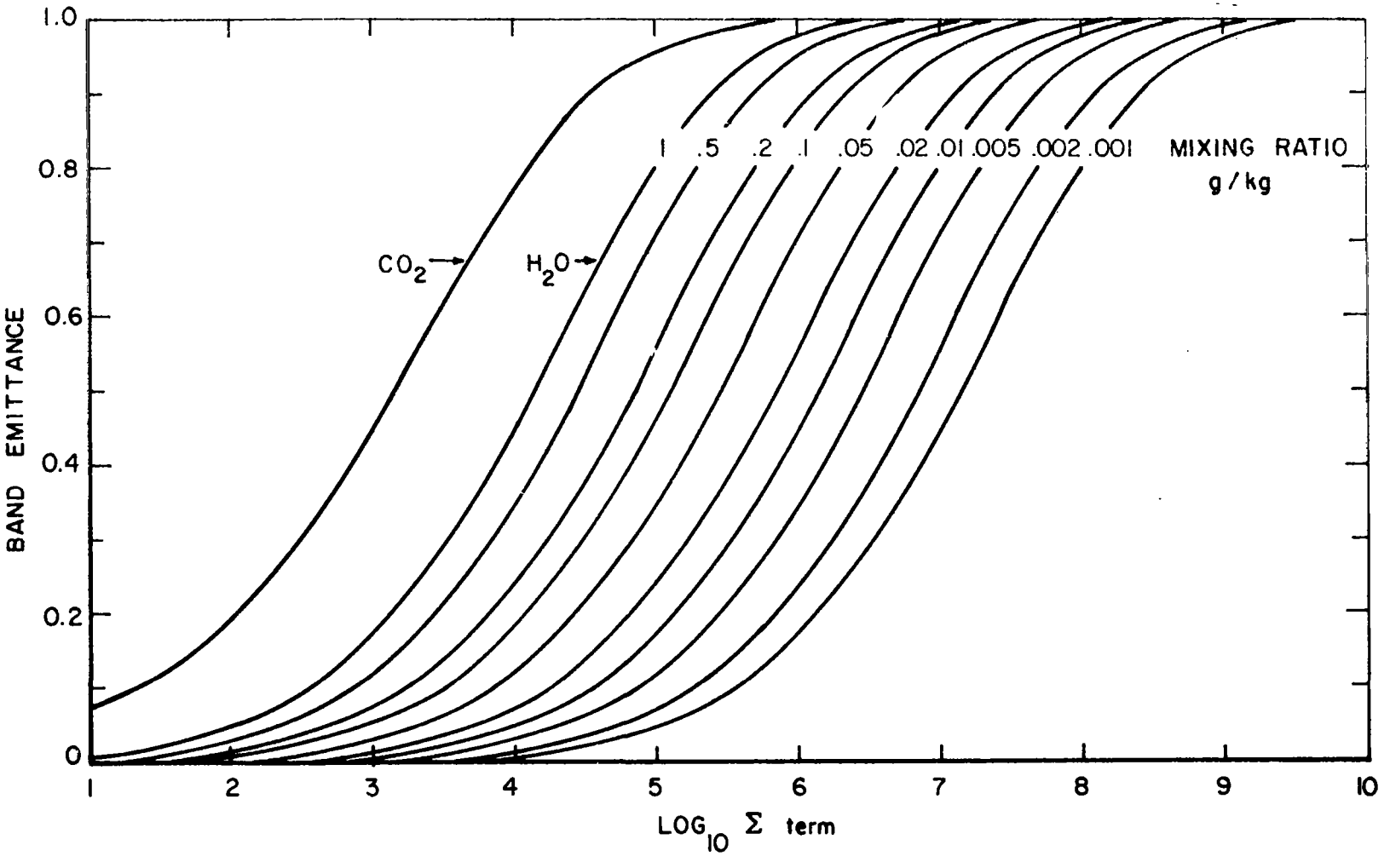

Figure 7. Variation in CO_2 band emittance for 615 to 715 cm^{-1} and H_2O band emittance for 315 to 475 cm^{-1}. Family of H_2O curves shows different values of water vapor mixing ratio. Effective temperature is 233°K.

seen when examining observed horizon radiances. The rise in the CO_2 profile occurs in the 30-km tangent height range, and the increase in the H_2O radiances occurs at about 10 km (see figure 1). Ideally the increase in the two radiance profiles should coincide in the same range of tangent heights. This may be accomplished by shifting the CO_2 band-pass filter to shorter wavenumbers (longer wavelengths). However, shifting the band-pass filter to more transparent regions of the CO_2 band entails some sacrifice of the signal-to-noise ratio at higher altitudes.

Summary Remarks

Analysis of the altitude dispersion characteristics of the horizon radiance in the CO_2 band indicates that the instant inversion technique will work for tangent heights greater than 20 km, and the accuracy should improve with altitude. It was shown that the emittance properties of the atmosphere appear to be linearly correlated with parameters characteristic of different air mass types. This property allows a calibration of the emittance for different climatological atmospheres and tangent height altitudes. Deviations from the condition of thermodynamic equilibrium are quite small and are of the order of 1 percent for horizon radiances at 60 km. Finally, it is shown from a comparison of CO_2 and H_2O band emittances that the spectral intervals of scanner observations are not matched for purposes of moisture inferences using both bands. However, the feasibility of the concept is demonstrated by noting that the shapes of the emittance curves are similar. What is needed is a radiometer designed to sense CO_2 emission in more transparent regions of the band, i.e., at shorter wavenumbers or longer wavelengths.

RESULTS

The instant inversion technique was applied to numerous horizon radiance profiles in the CO_2 band that were computed numerically on a digital computer. These test profiles were selected from NASA-CR66184 and NASA-CR66185 (ref. 13) so that the samples would represent the atmospheric variations over the full range of seasonal and geographical conditions. The technique was used to infer temperature structure in the 20 to 60 km tangent height range, and the resulting temperatures were compared with actual profiles used to compute the radiances. Statistics were compiled on the systematic error and random error uncertainties of several profile sets. These results allow a detailed evaluation of the instant inversion technique for inferring temperature structure.

The technique was then applied to two radiance profiles in the CO_2 band based on Scanner observations in order to illustrate its application to real data.

A detailed analysis of H_2O radiance profiles from Scanner observations was performed to estimate average radiances as a function of latitude. These average radiances were then inverted to determine moisture profiles at different latitudes within the geographical area of observation. An investigation was performed to determine the sensitivity of inferred water vapor mixing ratios to different transmittance models. Inferred moisture profiles include the tangent height range from 10 to 35 km.

Technique Evaluation

Criteria. - The instant inversion technique was applied to several independent sets of theoretical radiance profiles in the 615 to 715 cm^{-1} CO_2 band. Each selected set is noted by the following title:

(1) 30 GCA Profiles - selected from reference 13 by the investigators.

(2) 44 Aux. Profiles - the last 44 auxiliary profiles contained in NASA-CR66185 (ref. 13) which represent a collection of computed radiance profiles based on observed temperature and pressure profiles up to altitudes of 80 to 90 km.

(3) 36 Aux. Profiles - a selected sample of 36 profiles contained in the 44 profiles of (2).

(4) 30 LRC Profiles - a sample of 30 profiles provided by the scientists at the Langley Research Center. The origin of these profiles is unknown to the investigators of this report.

Statistics were compiled on the accuracy of the inferred temperature profiles for each sample set. Both the systematic error se(h) and random

error re(h) were determined for nine tangent height levels from 20 to 60 km. An entire set of calculations were performed for each of two emittance calibration parameters based on (1) the 10-mbar height and (2) the sum of nine radiances between the 20 and 60 km tangent height levels in increments of 5 km. Finally, statistical calculations were performed for three criteria of temperature comparisons; a comparison between the computed temperature and (1) the observed temperature at the 50-percent radiance level, (2) the average temperature over a 2-km layer centered about the level in question and (3) the average temperature over a 5-km layer centered about the layer in question.

Tables III and IV present tabulations of statistical results in terms of systematic and random temperature errors for 5-km layer comparisons. One obvious result from an inspection of systematic errors is a consistent underestimate of the temperature structure in the vicinity of the stratopause between 50 and 55 km. The error is on the order of 10° to 13°C too low.

The inability of the technique to predict temperature extremes follows from the approximations made in the theory. The assumption is made that the variation of the Planck radiance above a tangent height may be approximated by an average Planck radiance $\overline{B}_{\Delta\nu}[T(z')]$. Thus, in regions of the atmosphere where there are temperature maxima, the technique will consistently underestimate the temperature. Conversely, in regions of temperature minima, the technique will overestimate the temperature. Similarly, but to a lesser extent, in regions of the atmosphere where the temperature is increasing above the tangent height level, the technique will overestimate the temperature. Conversely, in atmospheric regions having a temperature lapse, the technique will underestimate the temperature.

A practical solution to the problem of overestimating or underestimating the temperature is to simply correct for the systematic error. This adjustment would be based on statistical averages of the required corrections for many radiance profiles.

It is noted that the systematic errors for 44 Aux. Profiles in Table III are all positive, considerably different than similar results for the 30 GCA Profiles. Each of the 44 profiles in this set was examined in detail to ascertain the reason for the difference. It was determined that eight of the 44 profiles were associated with arctic air masses having extremely cold temperatures in the troposphere and warm temperatures near the stratopause. These profiles were significantly different than any of the 20 climatological atmospheres used to calibrate the emittance as a function of air mass. Thus the computed emittances were too low in magnitude. Had these profiles been included in the calibration analysis, the emittances would have been approximated by a quadratic polynomial instead of a straight line as in equation (15).

After removing the eight profiles associated with arctic air masses, statistics were compiled for the remaining 36 Aux. Profiles. The resulting

TABLE III. — STATISTICAL EVALUATION OF INSTANT INVERSION TECHNIQUE

Emittance Parameter - 10 mbar Surface

Tangent Height h, km	30 GCA Profiles		44 Aux. Profiles		36 Aux. Profiles		30 LRC Profiles	
	se(h)	re(h)	se(h)	re(h)	se(h)	re(h)	se(h)	re(h)
20	1.9*	3.2*	2.4	4.2	3.6	3.6	1.5	2.2
25	2.8	2.3	3.6	3.3	4.4	2.7	1.4	1.9
30	2.1	3.4	2.3	3.0	2.7	2.6	1.0	1.6
35	0.8	1.5	0.5	3.8	-0.7	2.8	-1.6	2.3
40	-2.1	2.8	1.7	12.6	-3.7	4.6	-5.4	6.4
45	-5.5	4.9	3.3	25.8	-7.6	6.8	-7.2	4.7
50	-9.5	6.5	5.3	38.7	-10.6	8.3	-10.5	5.4
55	-12.3	7.2	7.4	52.1	-12.8	9.4	-10.5	5.6
60	-14.2	6.2	0.1	35.8	-14.4	8.6	-11.1	5.8

*Units of ^{o}C; se(h) - systematic error; re(h) - random error.

TABLE IV. — STATISTICAL EVALUATION OF INSTANT INVERSION TECHNIQUE

Emittance Parameter - Summed Radiances

Tangent Height h, km	30 GCA Profiles se(h)	30 GCA Profiles re(h)	44 Aux. Profiles se(h)	44 Aux. Profiles re(h)	36 Aux. Profiles se(h)	36 Aux. Profiles re(h)	30 LRC Profiles se(h)	30 LRC Profiles re(h)
20	2.0*	3.3*	2.2	4.9	3.7	3.9	2.0	2.3
25	3.0	2.6	2.9	5.2	4.8	3.4	2.7	2.2
30	2.5	3.7	0.6	6.9	3.2	4.3	3.4	1.5
35	1.3	3.1	-3.0	7.6	0.1	4.1	2.7	2.0
40	-1.4	3.5	-5.1	7.0	-2.5	4.3	1.1	5.5
45	-5.1	3.4	-7.9	5.7	-6.0	4.3	1.4	1.9
50	-8.4	2.7	-10.4	5.1	-8.8	3.8	-0.6	2.1
55	-11.3	2.3	-12.5	4.5	-11.1	3.4	-0.2	3.1
60	-13.3	2.0	-14.0	3.7	-13.0	2.6	-1.9	4.9

*Units of ^{o}C; se(h) - systematic error; re(h) - random error.

systematic errors are in excellent agreement with those for 30 GCA Profiles.

The systematic errors associated with the 30 LRC Profiles are different than the results of the other profile sets. This is especially true of the values presented in Table IV where the errors are slightly negative in the 50 and 60 km tangent height range. The key parameter to determine in the inversion solution is the total emittance at each tangent height. The results indicate that the profiles in this group are significantly different than those considered in the emittance calibration statistics. The problem encountered with these profiles is symptomatic of the eight arctic air masses in the 44 Aux. Profile set.

The inaccuracy of the emittance calibration is a major shortcoming of the instant inversion technique. One possible improvement that could be made is to develop a more sophisticated method of emittance calibration. Probably a more fruitful avenue to pursue is the development of an inversion technique which converges to a solution by the method of successive approximations. In this case, the emittance would be recomputed after each iteration until a solution is determined within the bounds of the instrumental error. An approach such as this would certainly overcome the inherent shortcomings of the present technique.

The random temperature error is a better indication of the prediction accuracy of the instant inversion technique, since it is possible to correct for systematic errors. Results in Table III based on the 10-mbar surface indicate random errors of about 2 to 3°C for the 20 to 40 km altitude range. This error is much larger in the vicinity of the stratopause and may be attributed to a poor statistical coupling between the height of the 10-mbar surface and atmospheric structure above 50 km.

Results in Table IV are more promising than those in Table III. Random errors have magnitudes on the order of 3 to 4°C for all altitudes tested, and there is an indication that the temperature accuracy improves for higher tangent heights. Even the results for the 44 Aux. Profiles are reasonable even though the aforementioned arctic air masses were included as part of the data sample.

Statistical results were determined for three criteria of temperature comparisons - a comparison between computed temperatures and the observed temperature at the same level, and the average temperature over 2 and 5 km layers in the atmosphere. The change in random errors for the three criteria are presented in Table V. As can be seen from the results, the random error increases about 0.5°C when going from a 5-km layer to a point-by-point comparison. The fact that the instant inversion technique predicts temperature as well as it does may be attributed to the geometry of limb-viewing and the peaked nature of the weighting functions.

TABLE V. — RANDOM ERRORS FOR THREE CRITERIA OF TEMPERATURE COMPARISONS

Parameter - Summed Radiances

Tangent Height h, km	30 GCA Profiles			36 Aux. Profiles			30 LRC Profiles		
	Point	2 km	5 km	Point	2 km	5 km	Point	2 km	5 km
20	4.4*	4.1*	3.3*	4.3	4.2	3.9	2.7	2.4	2.2
25	2.8	2.7	2.6	3.6	3.5	3.4	2.4	2.4	2.1
30	4.4	4.2	3.7	5.0	4.8	4.3	1.7	1.6	1.4
35	3.5	3.3	3.1	4.4	4.3	4.1	2.1	2.0	1.8
40	3.8	3.7	3.5	4.6	4.5	4.3	2.2	2.1	1.6
45	4.2	4.1	3.4	4.7	4.6	4.3	1.9	1.9	1.5
50	2.7	2.7	2.7	3.8	3.8	3.8	1.3	1.3	1.5
55	2.4	2.3	2.3	3.5	3.4	3.4	2.4	2.4	2.4
60	2.0	2.0	2.0	3.3	3.0	2.6	4.3	4.3	4.2

*Units of ^{o}C.

Temperature Inferences from Scanner Observations

The instant inversion technique was used to invert observations of horizon radiance in the CO_2 band in order to illustrate its application to realistic data. The data were extracted from a report (ref. 8) and are associated with average measured radiance profiles for Cells No. 4 and 7. The radiances were inverted and then corrected for systematic errors according to the results in Table IV. The inferred temperatures are compared to those temperatures deduced from meteorological analyses for the Scanner Mission. The agreement is good, and the temperature error is in line with the magnitudes of random errors presented in Table IV.

Moisture Inferences from Scanner Observations

It was mentioned in the discussion of the results of figure 7 that the spectral intervals for CO_2 and H_2O on the Scanner flight are not optically matched for purposes of inversion. Observations of the H_2O horizon radiance profiles are available in the 10 to 35 km tangent height range. Unfortunately, temperature inferences using the instant inversion technique from the CO_2 band are not applicable below the 30-km level. Therefore, it is not possible to perform every detail indicated by the development of the inversion theory.

In order to perform the inversion of H_2O radiance profiles, it is necessary to know the emitting temperature and the $\sum$ term in equation (13). Normally these parameters would follow as results from the inversion of CO_2 radiances. The magnitude of these terms in the mixing ratio computation [equation (14)] were determined from available temperature and pressure data (ref. 8) associated with the observed profiles. The effective temperature was computed as an average, weighted by the density along the line-of-sight, and the $\sum$ term was computed using the formulation of equation (11).

Analysis of Scanner Data. - The geographical coverage of the Scanner measurements is indicated by the hatched area of figure 10 - also shown are the nephanalysis and significant weather at time of observation. In reference 8 the radiance profiles were partitioned into seven geographical cell locations which vary as a function of latitude along the geographical annulus of observation.

An analysis was performed during the course of this study to determine average horizon radiances for the 315 to 475 cm^{-1} H_2O band as a function of latitude. Average radiance observations for this band were

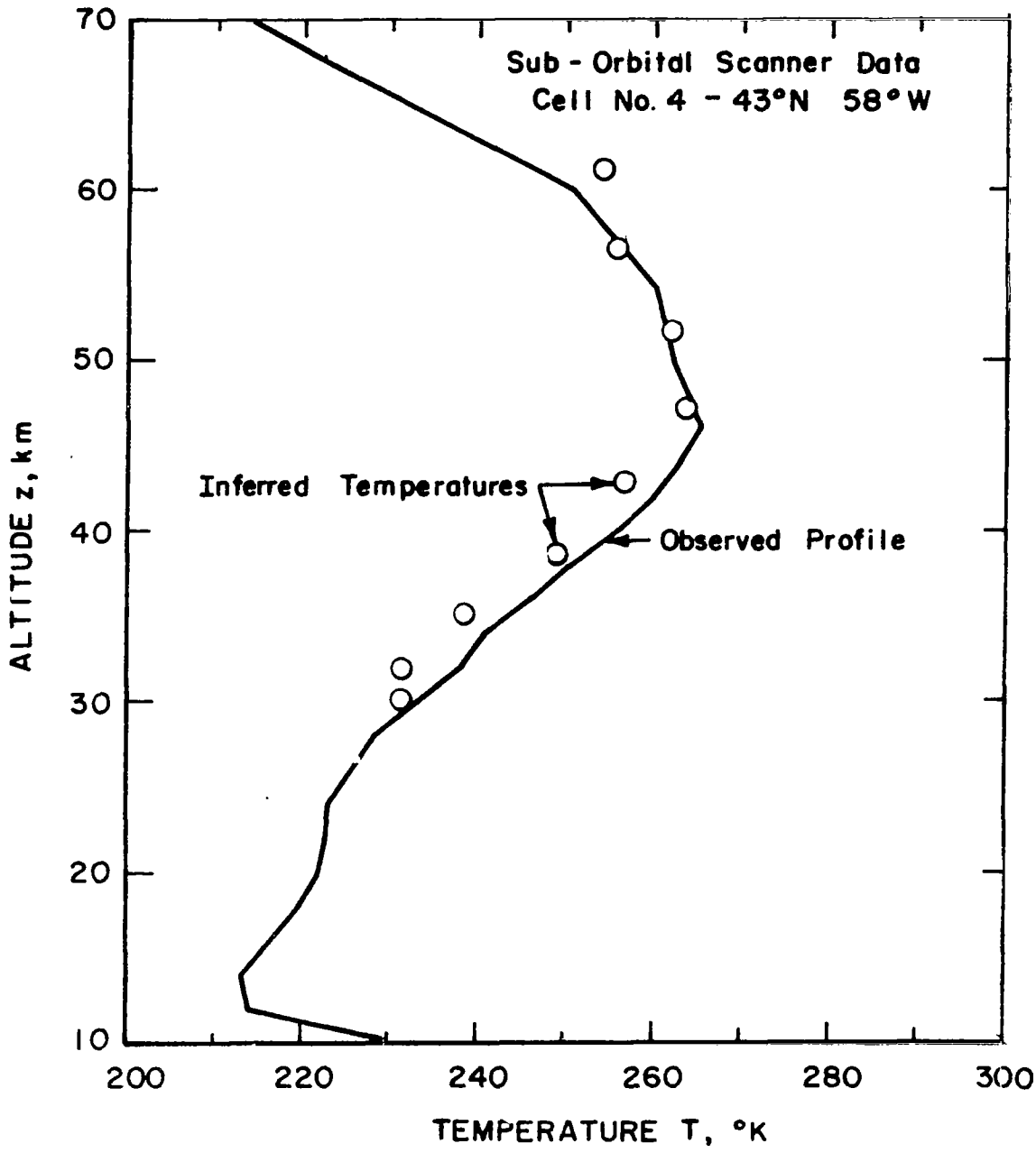

Figure 8. Comparison of inferred temperatures with the observed profile for Cell No. 4 of Scanner data.

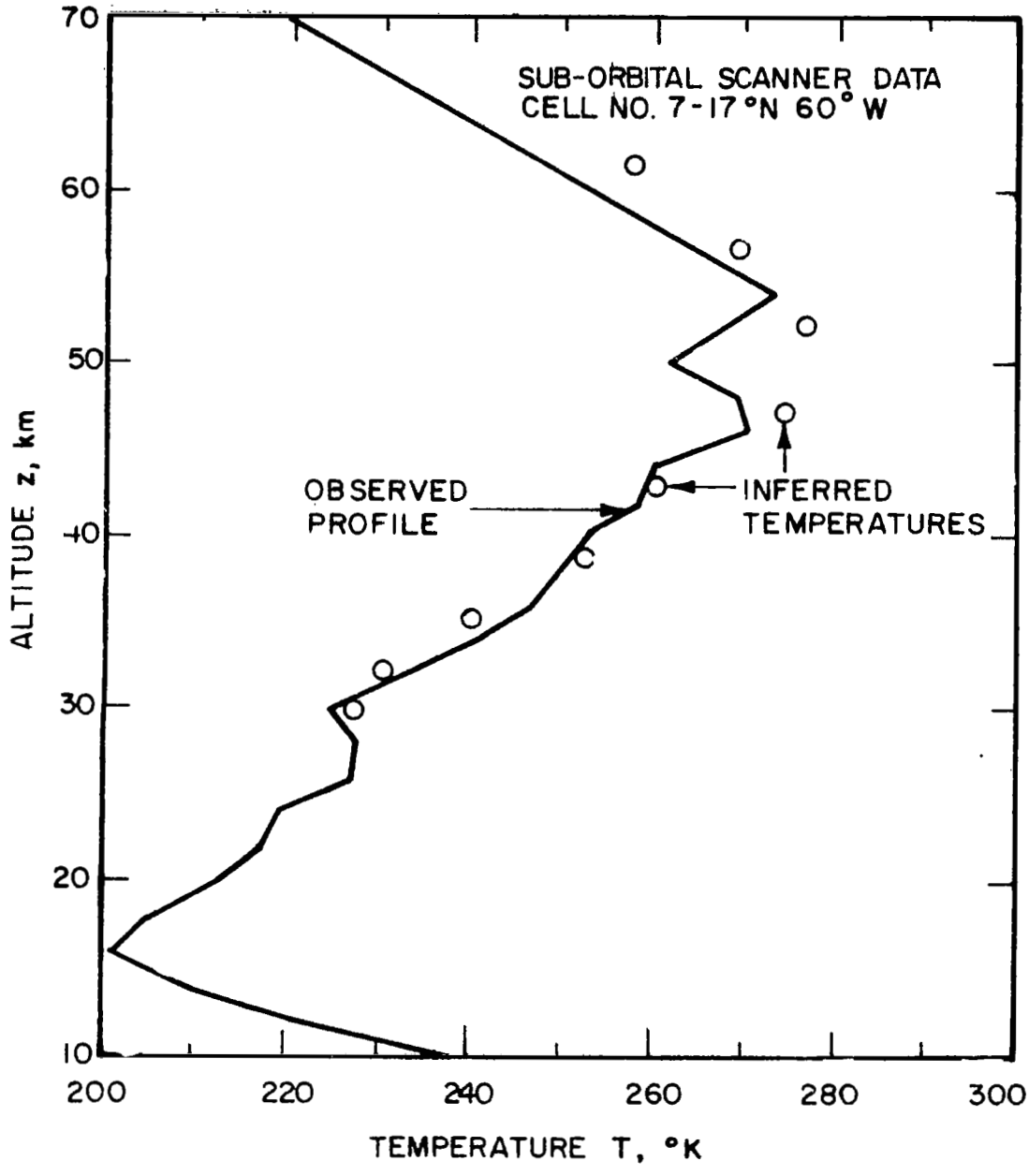

Figure 9. Comparison of inferred temperatures with the observed profile for Cell No. 7 of Scanner data.

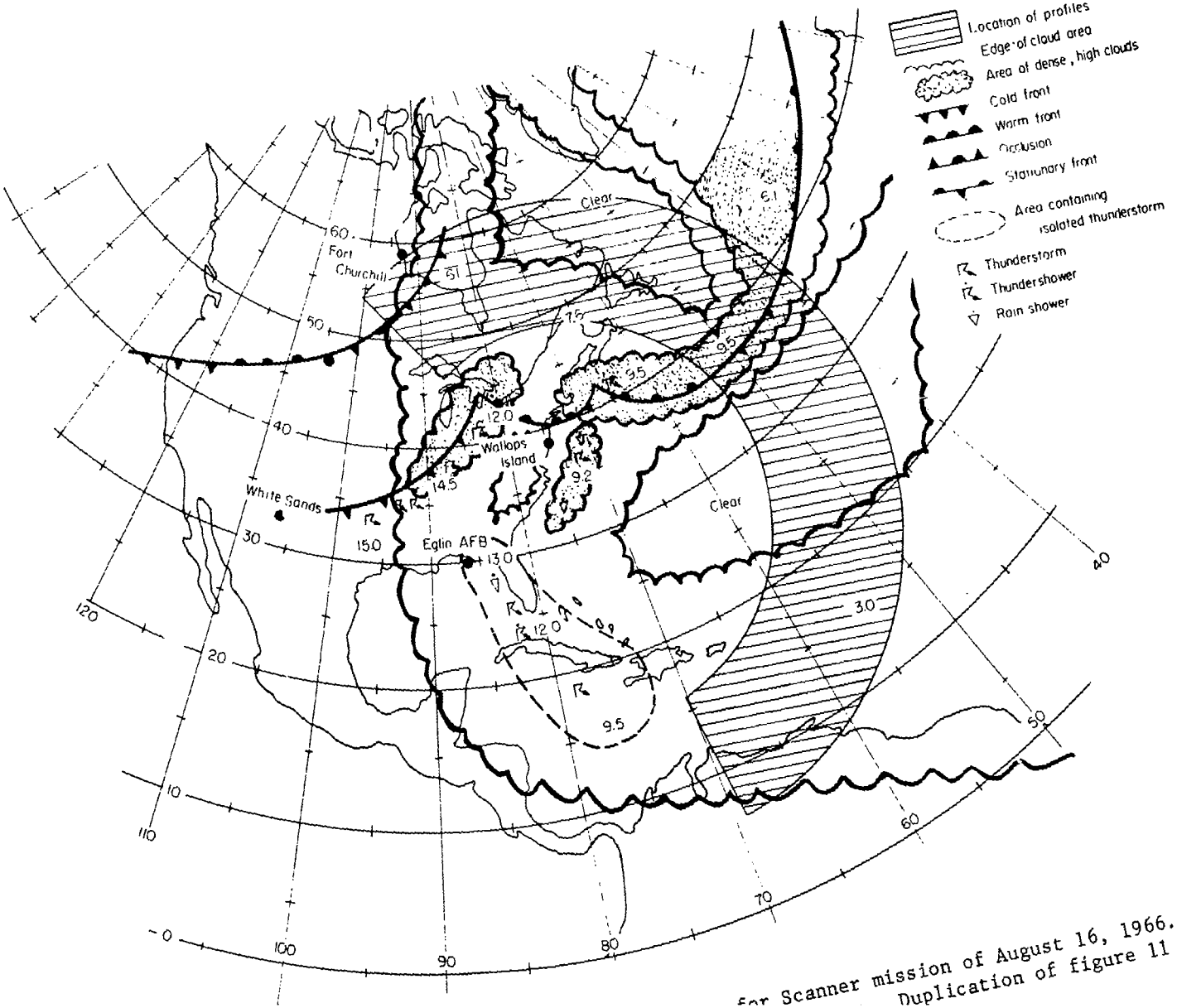

Duplication of figure 11 in ref. 8. Heights for Scanner mission of August 16, 1966.

plotted in figure 11 for six tangent height levels from 10 to 35 km. Trend lines drawn through the scatter of points, and radiance magnitudes were determined for the latitude position associated with each cell. Resulting average measured radiance profiles are tabulated in Table VI.

The average radiances for the 10 km tangent height should be viewed with some caution. The discussion in reference 8 indicates that both high level clouds and instrument response could introduce systematic biases into the magnitudes of the 10 km radiances. These bias factors have a tendency to lower the magnitude of observed radiances which in turn would result in decreased magnitudes of computed mixing ratios. Even with this qualification, however, the computed mixing ratios appear to have reasonable magnitudes.

Effective emitting temperatures were derived from model atmospheres developed (ref. 8). These temperatures were then converted to Planck radiances [equation (2)] representative of the 160 cm^{-1} band-pass at a central wavenumber of about 370 cm^{-1}. This wavenumber is shifted 25 cm^{-1} off the center of the band-pass filter to account for the asymmetry of the H_2O band within the 315 to 475 cm^{-1} spectral interval. Results are presented in Table VII.

Comparison of transmittance models. - An investigation was performed to determine the sensitivity of the inferred moisture profiles to different transmittance models. This analysis was based on a comparison of Elsasser's model (ref. 12) and that of Smith (ref. 14). Calculations of H_2O band emittance were made for a variety of mixing ratio profiles using the Standard Atmosphere temperature profile for both transmission models. The results are presented in the graphs of figure 12 where the band emittance is plotted as a function of U^*_H [equation (12)] on log-log scales. It is noted that Smith's model yields smaller values for emittances greater than 0.06 and larger values for emittances smaller than 0.06 in magnitude. An emittance of 0.06 corresponds to a tangent height of roughly 25 km. The emittance model can have a pronounced effect on the inference of moisture profiles in both the lower and upper stratosphere as will be shown in the next section. Smith's emittance model was used to compute moisture profiles for this study since it is based on recent calculations and has a finer spectral resolution than Elsasser's model.

Inferred moisture profiles. - Calculations of the water vapor mixing ratio were performed using the data in Tables VI and VII, Smith's transmittance model in figure 12 and equation (14). The results are presented in Table VIII for the seven cells. An average of the mixing ratios is shown in the last column. Computed mixing ratios indicate a general decrease to about 0.006 g/kg in magnitude at the 23-km level, a gradual increase to about 0.009 g/kg at 32 km and then a decided decrease to about 0.005 g/kg at 37 km.

The results in Table VIII are plotted in terms of latitudinal variations in figure 13. Some cautious conclusions may be drawn from these

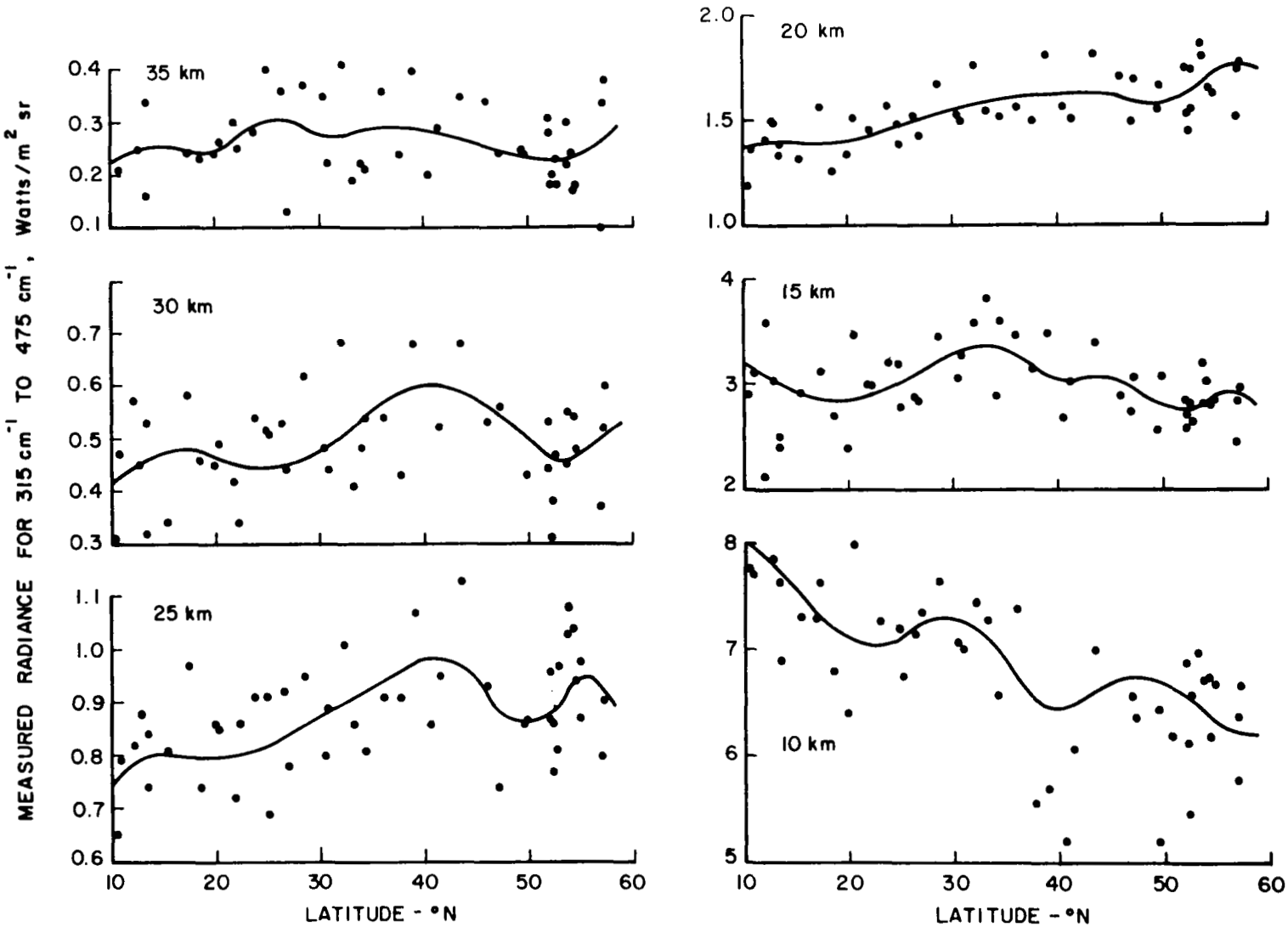

Figure 11. Average radiances in the H_2O band (315 to 475 cm^{-1}) from Scanner observations. Trend lines were drawn by band.

TABLE VI. — AVERAGE MEASURED RADIANCE PROFILES FOR 315 CM^{-1} TO 475 CM^{-1}

Tangent Height, km	Radiance $N_H(h)$, watts/m^2-sr (eq. 8)						
	Cell 1 58°N	Cell 2 53°N	Cell 3 47°N	Cell 4 43°N	Cell 5 35°N	Cell 6 21°N	Cell 7 17°N
10	6.20	6.50	6.70	6.60	6.90	7.10	7.30
15	2.80	2.80	2.90	3.10	3.30	2.90	2.80
20	1.74	1.64	1.59	1.63	1.60	1.42	1.40
25	0.90	0.90	0.89	0.97	0.93	0.79	0.80
30	0.51	0.46	0.55	0.59	0.55	0.46	0.48
35	0.28	0.23	0.25	0.27	0.29	0.26	0.25

TABLE VII. — EFFECTIVE EMITTING TEMPERATURES AND PLANCK RADIANCES FOR SCANNER OBSERVATIONS FROM 315 CM^{-1} TO 475 CM^{-1}

Tangent Height, km	Temperature, °K / Planck Radiance $B_H[T(z')]$, watts/m^2-sr (eq. 8)						
	Cell 1 58°N	Cell 2 53°N	Cell 3 47°N	Cell 4 43°N	Cell 5 35°N	Cell 6 21°N	Cell 7 17°N
10	224.0 / 9.89	223.1 / 9.78	223.4 / 9.82	219.6 / 9.27	220.9 / 9.53	223.1 / 9.78	223.1 / 9.78
15	225.5 / 10.07	224.2 / 9.92	220.8 / 9.52	218.6 / 9.26	215.7 / 8.96	207.8 / 8.08	207.7 / 8.07
20	228.2 / 10.39	227.4 / 10.30	226.6 / 10.20	224.5 / 9.95	222.4 / 9.70	219.1 / 9.32	218.9 / 9.30
25	234.6 / 11.14	231.2 / 10.74	231.8 / 10.81	230.9 / 10.70	230.2 / 10.63	229.4 / 10.53	229.0 / 10.48
30	240.9 / 11.93	240.3 / 11.86	241.1 / 11.95	240.9 / 11.93	239.1 / 11.70	237.1 / 11.46	235.6 / 11.26
35	250.6 / 13.14	249.3 / 13.00	249.6 / 13.04	249.9 / 13.08	251.5 / 13.24	250.6 / 13.14	250.4 / 13.12

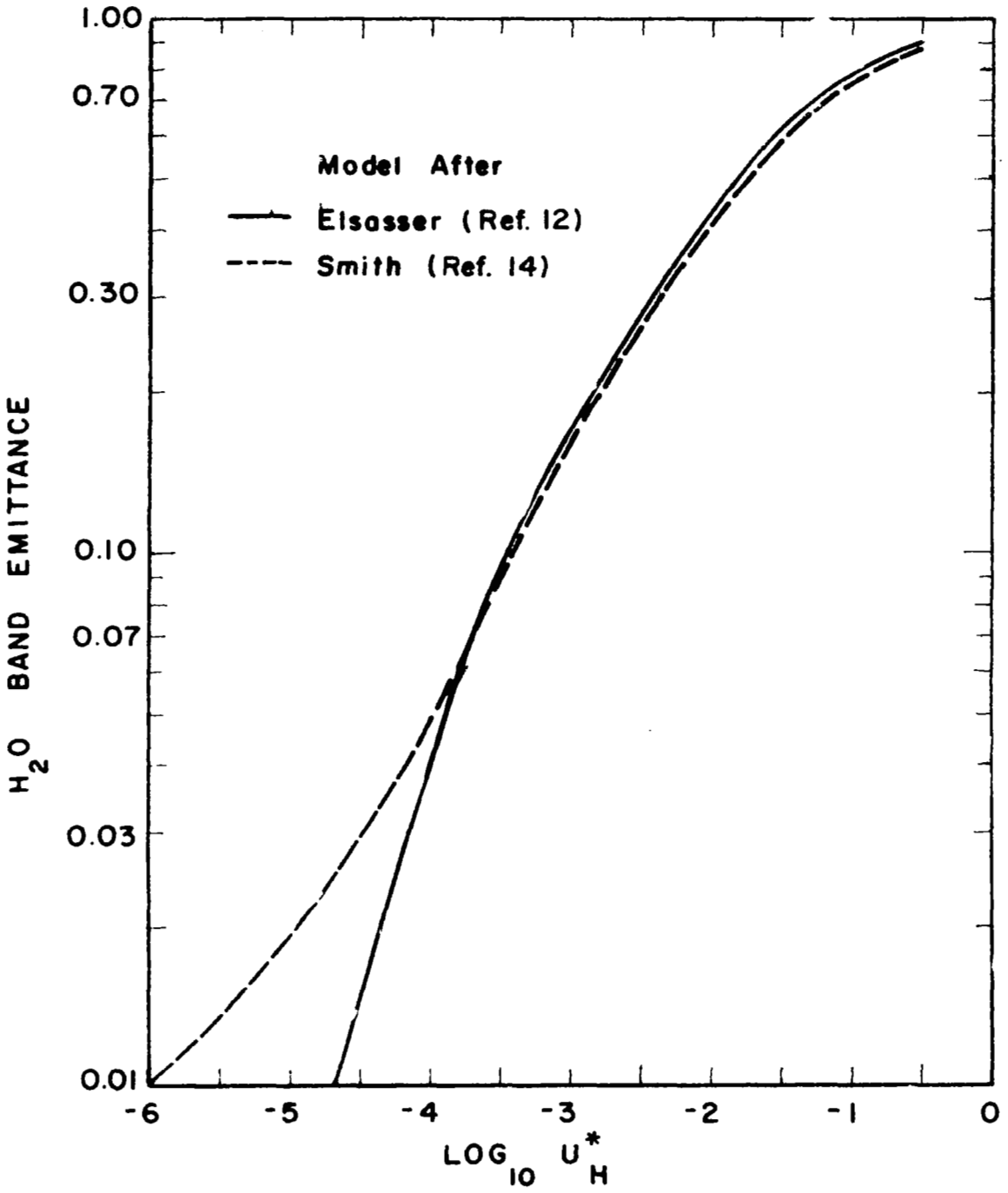

Figure 12. Comparison of H_2O band emittances (315 to 475 cm^{-1}) for two transmission models.

TABLE VIII. – INFERRED WATER VAPOR MIXING RATIOS FROM SCANNER OBSERVATIONS

Effective Altitude, km	Mixing ratio W_H, g/kg							
	Cell 1 58°N	Cell 2 53°N	Cell 3 47°N	Cell 4 43°N	Cell 5 35°N	Cell 6 21°N	Cell 7 17°N	Mean Values
14.9	0.0105	0.0145	0.0166	0.0178	0.0204	0.0195	0.0224	0.0174
18.6	0.0044	0.0046	0.0055	0.0071	0.0095	0.0089	0.0081	0.0069
22.8	0.006	0.0059	0.0058	0.0068	0.0069	0.0060	0.0059	0.0062
27.2	0.0068	0.0076	0.0071	0.0087	0.0066	0.0066	0.0068	0.0072
31.8	0.0076	0.0063	0.0089	0.0112	0.0105	0.0078	0.0089	0.0087
36.6	0.0051	0.0034	0.0036	0.0054	0.0063	0.0050	0.0042	0.0047

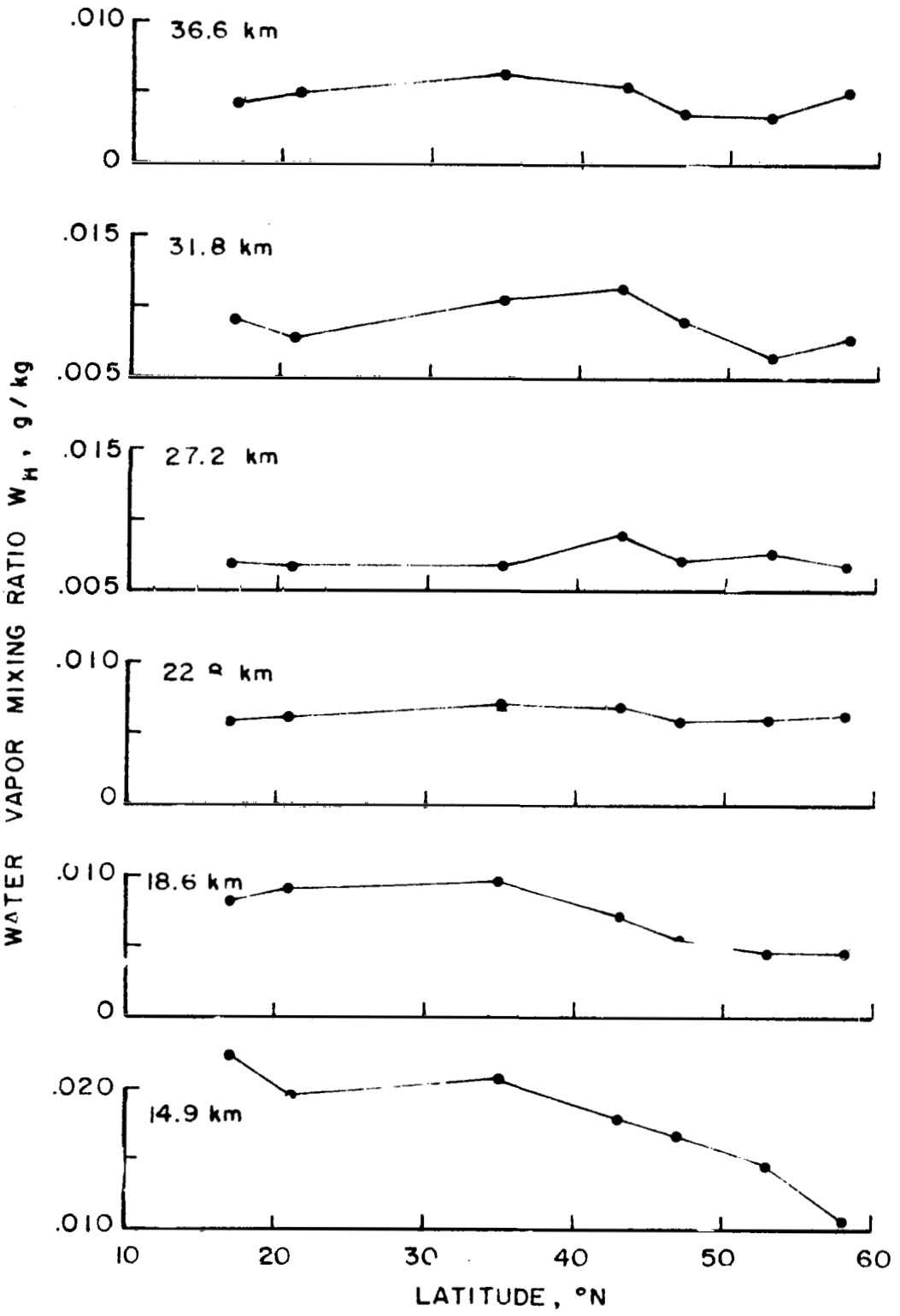

Figure 13. Latitude variation of water vapor mixing ratio as a function of emitting altitude using Smith's transmission model (ref. 14).

trend curves. Latitudes north of 45 degrees are consistently drier than those to the south. The subtropical region is quite moist up to about 20 km; however, the zone between 35 and 45°N is wettest above the 20-km level. It is interesting to note that this region is associated with a frontal weather situation in the troposphere (see figure 10). One may speculate that the weather activity has injected moisture into the stratosphere.

Figure 14 shows a comparison of mean mixing ratio profiles for two transmittance models. The results of Table VIII were based on Smith's transmittance model - similar calculations were performed in order to determine a mean profile for Elsasser's model. It is interesting to compare these profiles with the emittance curves in figure 12. The two profiles cross at an altitude of 27 km, which corresponds to the same intersection of the emittance curves. Above this level, larger emittance values yield small magnitudes of mixing ratio, and the converse is true for altitudes below 27 km.

The mixing ratios derived by this technique are generally larger in magnitude than typical values of between 0.002 and 0.003 g/kg observed by Mastenbrook (ref. 15) for the 25 to 30 km altitude range. However, some of his observations are considerably larger than the magnitudes derived here. It is difficult to establish at this time whether the inferred moisture profiles are too large in magnitude since independent measurements are not available at the time of observation.

Summary Remarks

The instant inversion technique was evaluated statistically using three independent sets of radiance profiles. Results indicated that the technique consistently underestimated temperature maxima and overestimated temperature minima. However, it is possible to correct inferred temperatures for systematic errors by adding or subtracting a given magnitude of temperature based on an average for all sets of profiles. Random temperature errors were of the order of 3 to 4°C for each set of profiles. The random error will increase to about 5°C if the uncertainty in the systematic error correction is included in the calculations. The instant inversion technique works quite well in view of its simplicity of approach. The technique was successfully applied to observed horizon radiances from Project Scanner in both the CO_2 and H_2O rotational bands.

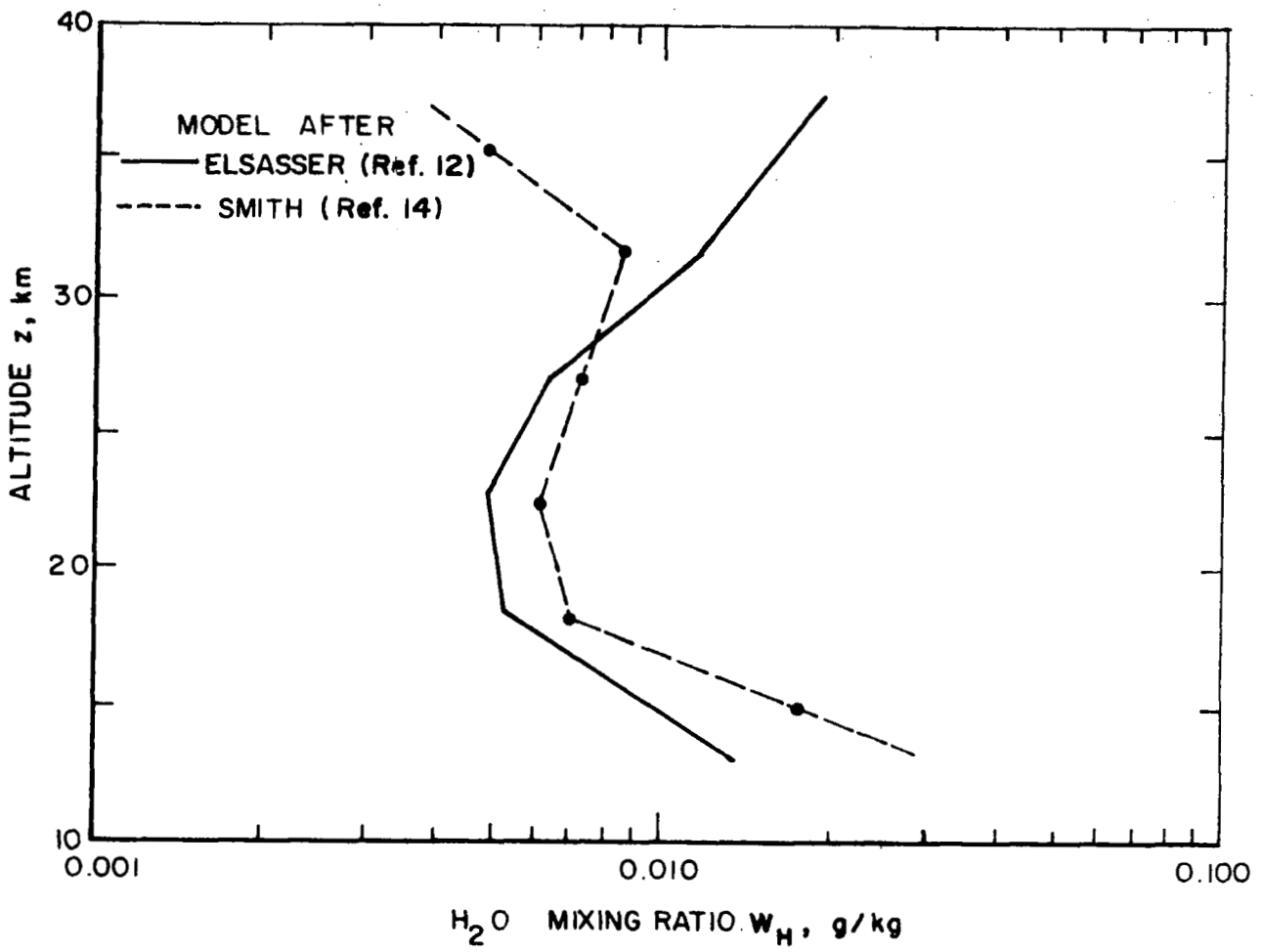

Figure 14. Comparison of mean mixing ratio profiles inferred from horizon radiances measurements 315 to 475 cm^{-1} (ref. 8) for two transmission models.

SUMMARY ANALYSES

Part of the effort under this program was directed toward an analysis of errors pertinent to the inference of temperature and moisture from horizon radiance measurements. This task was approached by considering representative errors of radiometer systems that could be flown on earth-orbiting spacecraft. Calculations were based on the formulation specified by the instant inversion technique. Random error uncertainties were estimated for both temperature and moisture inferences as a function of altitude in the atmosphere.

Analyses were also performed to determine optimum spectral intervals in the H_2O and CO_2 rotational bands for radiometer systems to be used for purposes of temperature and moisture inferences.

Results of these analyses are presented in this section of the report.

Achievable Temperature Inference Accuracies

It has been demonstrated that the instant inversion technique is a reasonably good predictor of temperature and moisture profiles. Since the formulation is simple, it is quite useful in performing error analyses of prediction accuracies. There are two sources of observational errors — radiance measurement errors and uncertainties in specifying the tangent height altitude. There are also errors associated with the emittance $\epsilon(h)$ or transmission model used in the calculations and errors in the inversion technique itself. It is reasonable to neglect errors due to the inversion scheme since an iteration approach with regression analyses will certainly overcome the shortcomings of the instant inversion technique. Differentiating equation (5) gives

$$dT(h)\,\frac{\partial \bar{B}}{\partial T} = \frac{dN(h)}{\epsilon(h)} + \frac{1}{\epsilon(h)}\,\frac{\partial N(h)}{\partial h}\,dh - \frac{N(h)}{\epsilon(h)^2}\,d\epsilon(h) \qquad (17)$$

Assuming these errors are uncorrelated, the rms temperature error is expressed by

$$\Delta T(h)_{rms} = \left(\frac{\partial \bar{B}}{\partial T}\right)^{-1} \frac{1}{\epsilon(h)} \left[\Delta N(h)^2 + \left(\frac{\partial N(h)}{\partial h}\right)^2 \Delta h^2 + N(h)^2 \left(\frac{\Delta \epsilon(h)}{\epsilon(h)}\right)^2\right]^{1/2} \qquad (18)$$

A random radiance accuracy of 0.01 watts/m^2 sr and a tangent height error of Δh = 0.4 km are assumed to be reasonable for instrumentation on spacecraft. The random uncertainty in the emittance $\epsilon(h)$ was estimated to be about 2 percent $\left(\frac{d\epsilon(h)}{\epsilon(h)} = 0.02\right)$. These values along with total emittances

and radiances for the Standard Atmosphere in the 615 cm^{-1} to 715 cm^{-1} spectral range were substituted in equation (18) to obtain estimates of the rms temperature error. The results are presented in figure 15.

Errors are generally 1°C in the lower stratosphere, increase gradually to about 4°C near the stratopause and further to about 5°C at the 60-km level. The accuracy of the tangent height level is the principal contributor to the rms temperature error between 20 and 55 km, and the measured radiance accuracy becomes the dominant source of error above the 60-km level. These estimated rms temperature accuracies are certainly competitive with those from meteorological rocket soundings. Wagner (ref. 16) indicates temperature errors on the order of 5°C to 9°C in the 50 to 60-km altitude range for bead thermistor sensors used by the Meteorological Rocket Network.

It may be argued that the determination of the tangent height is more systematic than random in character for an individual profile. This follows from an argument that the spacecraft's attitude may be uncertain by about 0.4 km; however, this uncertainty may be constant over the time interval of measurement (less than 1 sec). If this situation is realistic, the entire radiance profile is in error by a systematic increment of tangent height. In a corresponding manner, the inferred temperature profile may be shifted by a similar error in the altitude from of reference. On this basis the temperature gradients with altitude may be quite accurate, but the absolute temperature at a given level will be in error by magnitudes indicated in the analysis.

Possible verification of this systematic error and its effect on temperature accuracies could be accomplished in a more detailed analysis of the problem.

Achievable Moisture Inference Accuracies

Estimates of the prediction accuracies of water vapor mixing ratio may be determined by an approach similar to that used for temperature accuracies. From equations (8) and (10),

$$\tau_H(h) = 1 - \frac{N_H(h)}{\overline{B}_H(h)} \tag{19}$$

Differentiating equation (19) gives

$$d\tau_H(h) = \left[- \frac{dN_H(h)}{\overline{B}_H(h)} + \frac{1}{\overline{B}_H(h)} \frac{\partial N_H(h)}{\partial h} dh + \frac{N_H(h)}{\overline{B}_H(h)^2} dB_H(h) \right] \tag{20}$$

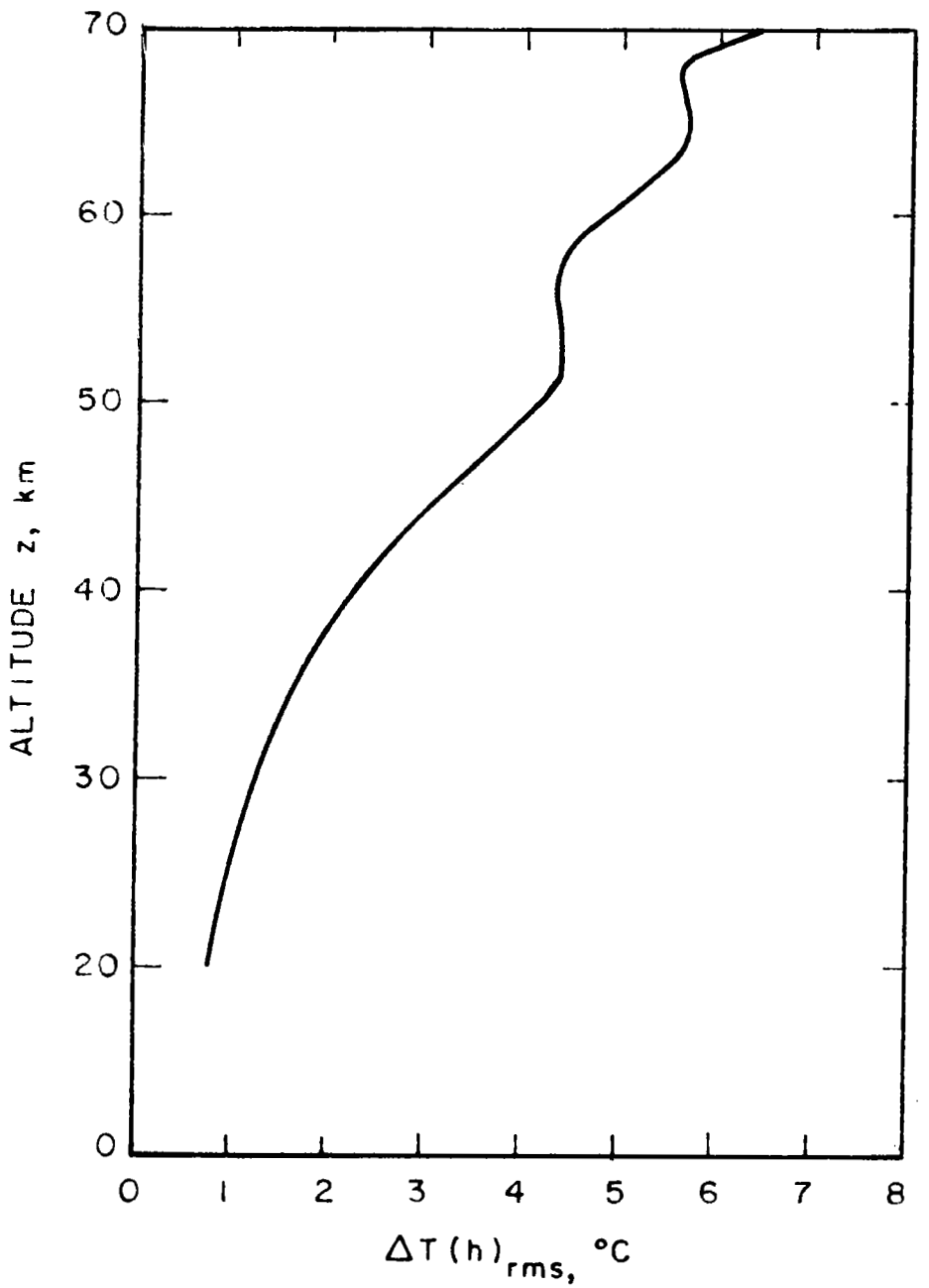

Figure 15. Computed rms temperature errors as a function of altitude.

Assuming the transmittance is approximated by the following exponential form

$$\tau_H(h) = \exp\left(-W_H \sum\right) \tag{21}$$

differentiation gives

$$d\tau_H(h) = -\sum \tau_H(h)\, dW_H \tag{22}$$

From equation (21)

$$W_H = \frac{\ell n\left(\frac{1}{\tau_H(h)}\right)}{\sum} \tag{23}$$

Combining equations (22) and (23)

$$\frac{dW_H}{W_H} = -\frac{d\tau_H(h)}{\tau_H(h)\ \ell n\left(\frac{1}{\tau_H(h)}\right)} \tag{24}$$

Assuming the errors are uncorrelated, the fractional rms mixing ratio error may be expressed from equations (20) and (24) by

$$\left(\frac{\Delta W_H}{W_H}\right)_{rms} = \frac{1}{\tau_H(h)\ \ell n\left(\frac{1}{\tau_H(h)}\right)} \frac{1}{\bar{B}_H(h)} \left[\Delta N_H(h)^2 + \left(\frac{\partial N_H(h)}{\partial h}\right)^2 \Delta h^2 + N_N(h)^2 \left(\frac{\Delta \bar{B}_H(h)}{\bar{B}_H(h)}\right)^2\right]^{1/2} \tag{25}$$

Equation (25) was evaluated over the altitude range from 10 to 50 km using realistic magnitudes of errors and input values. A random radiance accuracy of 0.025 watts/m^2 sr and a tangent height error of 0.4 km were assumed. Values for the transmittance $\tau_H(h)$, horizon radiances $N_H(h)$ and Planck radiances $\bar{B}_H(h)$ were extracted from the scanner data in tables VI and VII. Theoretical calculations of these parameters were used for data in the 35 to 50-km altitude range. Temperature errors (or $\Delta\bar{B}_H(h)$ errors) were based on data in figure 15. The results of the calculations are presented in figure 16 as percent errors of the absolute values of the mixing ratios.

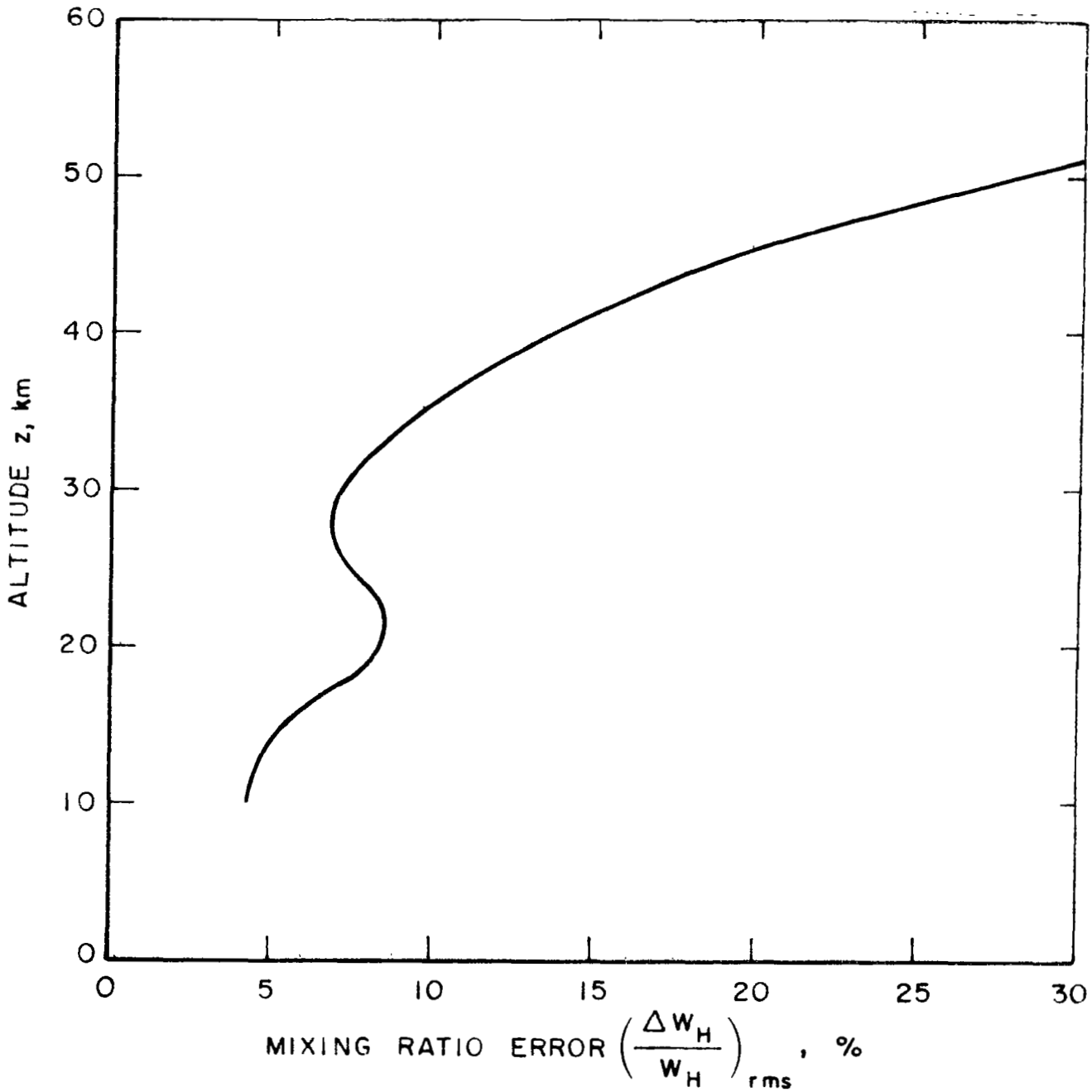

Figure 16. Computed rms mixing ratio errors as a function of altitude

RMS mixing ratio errors are generally 5 to 8 percent in the 10 to 30 km altitude range. The percent error increases consistently above the 30-km level to a value of 30 percent at 51 km. In order to obtain the absolute error from these results, the value of the mixing ratio is multiplied by the percentage for a given level. For example, a 20 percent error for a mixing ratio of 0.010 g/kg amounts to a rms uncertainty of 0.002 g/kg. If the mixing ratio were 0.002 g/kg, the rms error would be only 0.0004 g/kg.

The calculations indicated that the tangent height uncertainty in the 10 to 25 km altitude range was the prime source of error. This is the region of the H_2O radiance profile where the slope of the curve $(\partial N_H/\partial h)$ is greatest in absolute magnitude (see figure 1). Above 25 km, the radiance accuracy is the dominant source of error. The calculations also indicated that errors due to temperatures are relatively unimportant compared to radiance and tangent height errors. This means that the mixing ratio calculation is insensitive to temperature errors determined from CO_2 radiance profiles, and this result emphasizes the feasibility of using a dual radiometer system to obtain temperature and moisture profiles in the stratosphere.

Optimum Spectral Intervals

The general criterion that may be applied to the selection of bandpass filters is the maximum radiant power that could be intercepted by a radiometer (i.e., maximum signal-to-noise). A complete treatment of this problem would consider a detailed analysis of entire radiometer systems. The approach to the problem here is restricted in scope and considers only atmospheric physics, and thus disregards instrumental problems such as filter response and detector response.

CO_2 band. — Two factors influence the problem of selecting CO_2 bandpass filters: (1) maximum possible signal for measurements at high tangent height levels, and (2) an optical matching of the radiance profile associated with the H_2O band (see section on a Comparison of CO_2 and H_2O Band Emittances). The investigation approached the problem by considering optical path lengths as a function of tangent height, and then relating these to the optical properties of the band. It is also desirable to maintain the peaked nature of the weighting functions at all altitudes (see figure 3), which maximizes the inversion possibilities. These considerations led to the following suggestions for the selection of bandpass filters

(1) Single filter radiometer — spectral response 590 cm^{-1} to 700 cm^{-1}.
(2) Dual filter radiometer — spectral responses 615 cm^{-1} to 700 cm^{-1} and 570 cm^{-1} to 660 cm^{-1}.

The selection of the single filter is a compromise and attempts to fulfill the two requirements of maximum signal and optical matching.

The selection of two filters is quite attractive in that each filter optimizes a given altitude region of the atmosphere. The 615 cm^{-1} to 700 cm^{-1} filter applies to the 30 to 65-km altitude range, and the 570 cm^{-1} to 660 cm^{-1} filter provides good signals in the 10 to 40-km altitude range. The overlap in the 30 to 40-km range allows a continuity of measurements for purposes of temperature inferences.

It should be noted that the spectral region beyond 700 cm^{-1} is avoided due to the presence of a moderate ozone absorption band at 14 microns. Secondly, there is justification for extending the spectral response towards shorter wavenumbers in the wings of the H_2O band since there are relatively small path lengths of water vapor in the stratosphere, even when considering limb viewing. Reduced path lengths at 10 km are generally about 0.1 pr cm, an order of magnitude less than the total precipitable water concentration of a vertical column in the troposphere. Calculations of the radiance from water vapor in the 570 to 600 cm^{-1} spectral range indicate that the contribution by H_2O to the total radiance is on the order of 1 percent at 10-km tangent heights. Therefore, it is reasonable to extend the band-pass filter to 570 cm^{-1} in order to obtain maximum signal at altitudes of 10 to 15 km.

H_2O band. - Several factors can influence the selection of a band-pass filter in the H_2O rotational band. The principal factor is the optical properties of the band as a function of spectral region. Other factors such as effective emitting temperature, tangent height and width of the band-pass filter also influence the selection. It is emphasized again that the investigation here considers only the atmospheric physics part of the problem and disregards the instrument itself.

The investigation was approached by considering the detailed spectral emitting properties of the band from 200 to 600 cm^{-1} for a number of different atmospheres and water vapor concentrations. Calculations were based on equation (8), using Smith's transmittance model (ref. 14) to compute the emittance. The computed spectral radiances were smoothed by different band-pass filter widths of $\Delta\nu$ = 40, 80, 120, and 160 cm^{-1} in a manner which simulates what the radiometer would receive. These results were then analyzed to determine the optimum filter configuration as a function of tangent height. The study is limited to filters positioned in the 20μ to 35μ region, in accordance with the statement of work.

The calculations indicated that the spectral radiance over spectral widths $\Delta\nu$ of 5 cm^{-1} exhibits considerable fine scale structure as is indicated by the results in figure 17 for a 20-km tangent height. Spectral radiances like those in figure 17 were computed for tangent heights from the surface to 50 km in 5 km intervals, and for a variety of selected atmospheric conditions. These detailed radiances were smoothed, and figure 18 is an example of results when the radiances were smoothed with the four filter functions. The selection of the optimum central wavenumber for a band-pass filter is based on the region which gives the maximum radiant power.

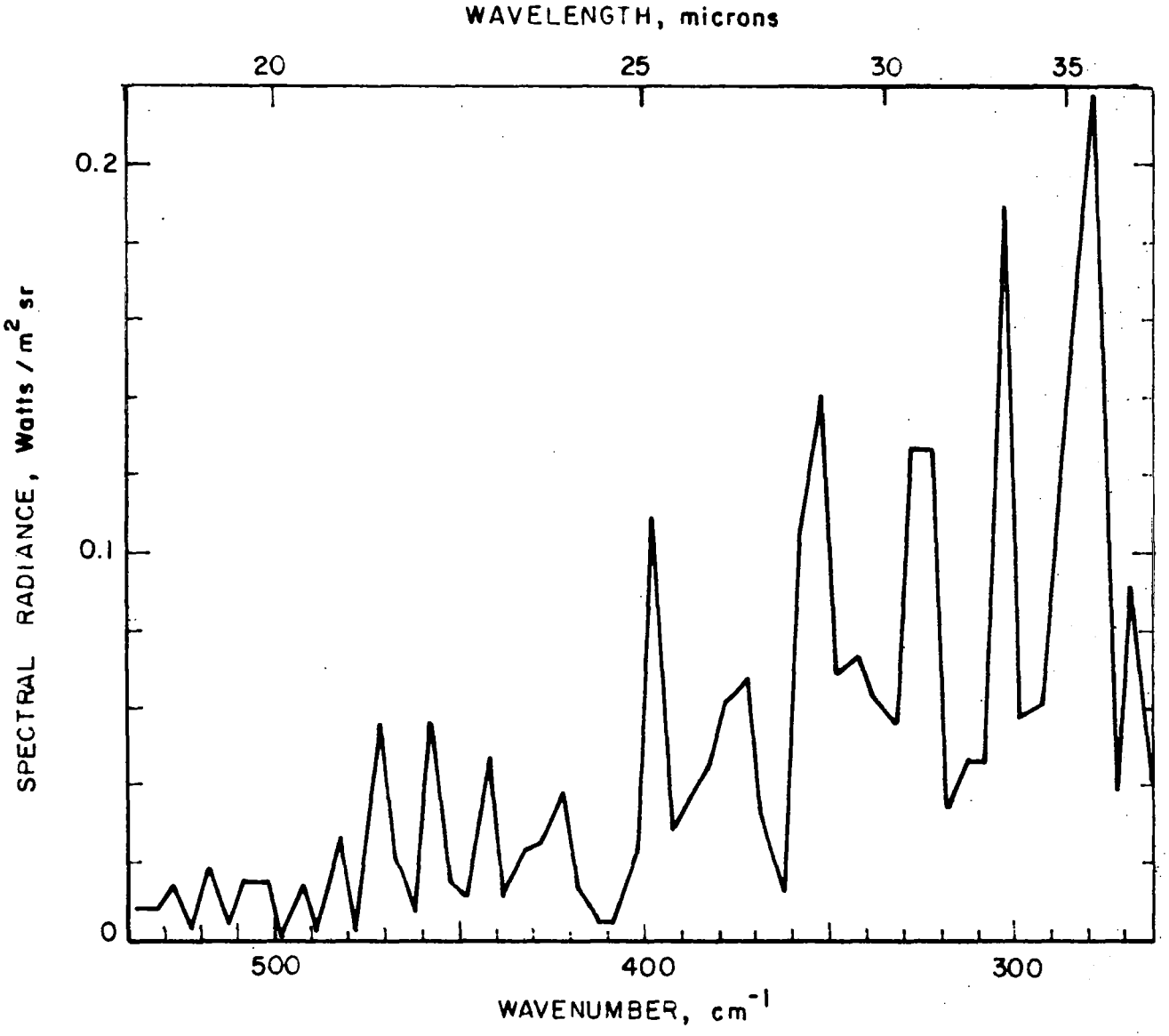

Figure 17. Variation in spectral radiance as a function of wavenumber for the H_2O rotational band. Spectral interval is $\Delta\nu$ = 5 cm^{-1}, and the tangent height is 20 km.

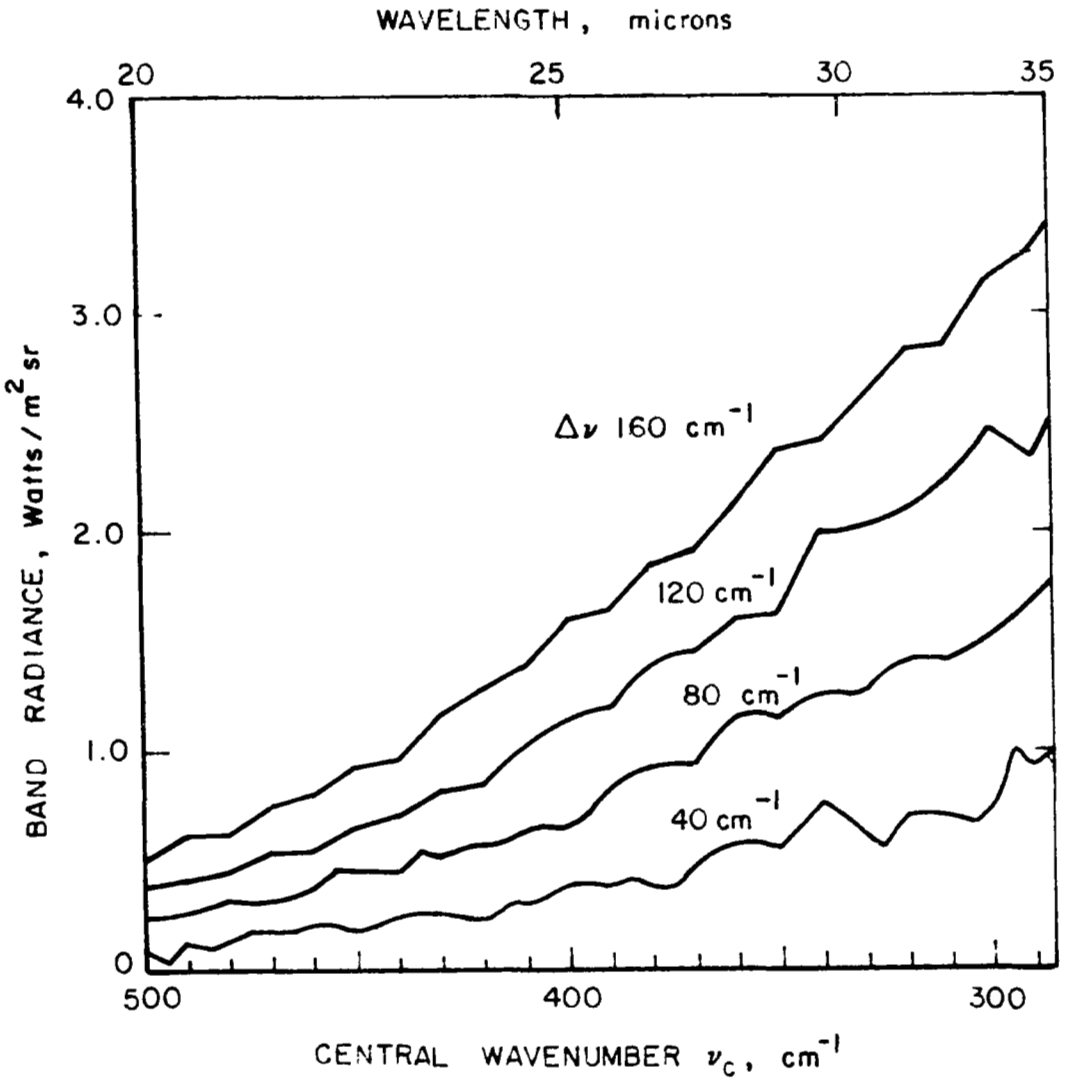

Figure 18. Smoothed radiance profiles for different band-pass filter widths. Radiances in figure 17 were used in these calculations and apply to a tangent height of 20 km.

The final results of this analysis are presented in figure 19 which indicates the filter position as a function of tangent height for the H_2O rotational band. For all practical purposes, the filter position is independent of band-pass width. The controlling factor in the altitude range from the surface to 15 km is the effective emitting temperature which manifests itself in terms of the nonlinear Planck radiance. This effect applies only in regions of the atmosphere where the optical path length is nearly opaque. As opacity decreases from near unity, the position of the filter rapidly moves to longer wavelengths. This characteristic is a result of the optical properties of the band.

It is concluded from this analysis that the band-pass filter should be positioned at 35μ or even longer wavelengths, if possible. This filter position provides the maximum radiant power to the radiometer and enhances the accuracy of inferred moisture profiles.

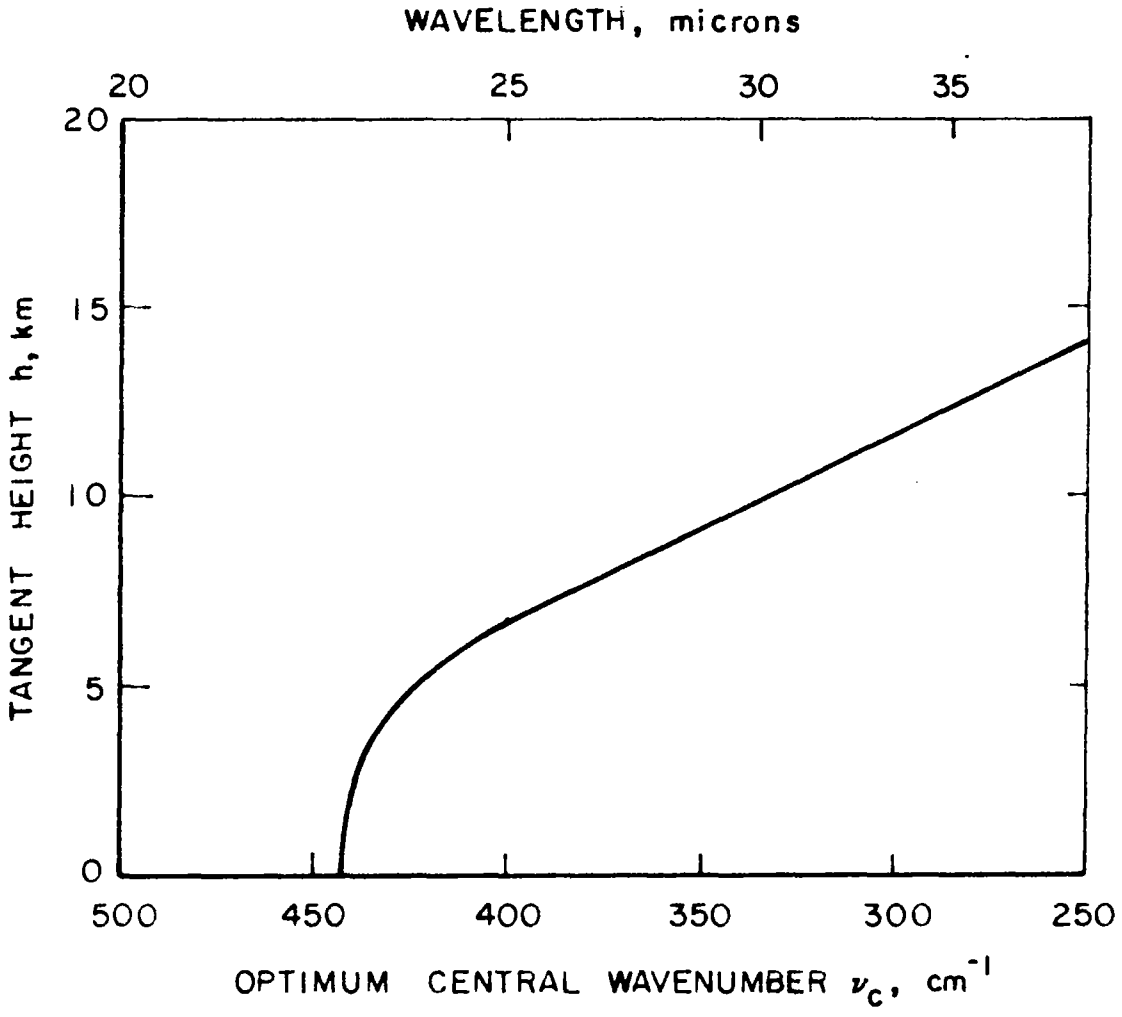

Figure 19. Variation in the optimum central wavenumber of a band-pass filter as a function of tangent height for the rotational water vapor band.

CONCLUDING REMARKS

A detailed investigation has been performed to assess the feasibility of inferring stratospheric temperature and moisture profiles from horizon radiance measurements. Both the 15μ CO_2 band and the H_2O rotational band were considered as potential spectral regions in the infrared whose radiance measurements can be used for temperature and moisture inferences. It was concluded that useful temperature measurements can be obtained from CO_2 band radiances over the altitude range from 10 to 65 km. Water vapor mixing ratios can be determined from H_2O band radiances for altitudes from about 10 to 50 km.

The optical properties of the CO_2 band (615 to 715 cm^{-1}) and the H_2O band (315 to 475 cm^{-1}) were studied in detail. An inference method termed the instant inversion technique was developed for both bands and then applied to theoretical profiles as well as observed radiance profiles from Project Scanner. There was good agreement between computed and observed temperature profiles, and the inferred magnitudes of water vapor mixing ratio were in general agreement with recent observations from balloons by frost-point hygrometers.

Statistical analyses of temperature inference results for approximately 100 sample profiles indicate that the instant inversion technique can predict temperatures to accuracies of about 5°C. The error is due principally to the estimation of total atmospheric emittance at a tangent height. This shortcoming may be eliminated by developing an inversion technique which converges to a solution by the method of successive approximations. The emittance would be recomputed after each iteration until a solution is determined within the bounds of the instrumental error. A similar iterative approach may be used to infer moisture profiles once the temperature profile is determined.

Analyses were performed to estimate temperature inference accuracies for realistic radiance profile measurements. Sources of random error included radiance measurements, tangent height error and uncertainties in the transmission model. Results indicate rms accuracies of about 1°C in the lower stratosphere, 4°C near the stratopause and 5°C at the 60-km level. The principal source of error was due to the tangent height determination. It may be argued that this error is more systematic than random in character for a given radiance profile which tends to reduce the random temperature error. Possible verification of this systematic error and its effect on temperature accuracies could be accomplished in a more detailed analysis of the problem.

A similar study was carried out to determine moisture inference accuracies. Sources of error included radiance measurements, tangent height error and uncertainties in the temperature inference. Results

indicate rms accuracies on the order of 5 to 8 percent in the 10 to 30 km altitude range, and the error increases to about 30 percent at the 50 km level. The absolute error is interpreted to be the product of the percentage and the absolute value of the mixing ratio. The tangent height error contributes to the inaccuracies in the lower altitude range, and the radiance error is dominant above 30 km. The calculations indicated that moisture estimates were insensitive to temperature errors.

Analyses were performed to determine the optimum spectral intervals in the infrared whose radiance measurements can be used to infer temperature and moisture profiles in the stratosphere. It was suggested that two band-pass filters be used when making the CO_2 radiance measurements, one with a spectral response 615 to 700 cm^{-1} and the second with a response of 570 to 660 cm^{-1}. These filters would apply to the upper and lower stratosphere, respectively. A single broad band-pass filter is required for the H_2O rotational band, and it should be centered at 35μ or even longer wavelengths, if possible.

Horizon radiance observations offer an attractive means to sound the stratosphere. Global measurements of stratospheric temperature and moisture profiles are not currently available for forecasting or research use. The results of this study have demonstrated the feasibility of making these measurements from earth-orbiting spacecraft. Furthermore, it should be possible to determine profiles of atmospheric ozone based on horizon radiance measurements in the 9.6μ band. Further studies should be directed toward the investigation of optimum inference techniques and specification of measurement requirements of instruments with the goal of developing the experiment for application on earth-orbiting spacecraft.

APPENDIX A

TEMPERATURE INFERENCE AND EVALUATION COMPUTER PROGRAM

A computer program termed INVERT was developed during the course of the study effort and was used extensively to test and evaluate the instant inversion technique. The following four points described the program's capabilities and options.

(1) Evaluates up to 100 radiance profiles at once.

(2) Performs the instant inversion technique for
   (a) two spectral intervals 615-715 cm^{-1} and 600-725 cm^{-1},
   (b) two emittance calibration parameters,
   (c) two types of effective emitting levels.

(3) Computes temperature errors for the above combinations of parameters and for a
   (a) point temperature comparison,
   (b) 2-km layer average temperature comparison,
   (c) 5-km layer average temperature comparison.

(4) Compiles statistics of temperature errors for all combinations of parameters and for the following statistics:
   (a) the root-mean-square (rms) error,
   (b) the systematic error component of the rms error,
   (c) the random error component of the rms error.

INVERT is written in conventional FORTRAN II language and should operate without modification on most digital computers. The program is available for anyone desiring its use. Requests for source deck listing and operating instructions should be directed to the authors or to the technical monitor at LRC, Mr. R. E. Davis.

REFERENCES

1. Baumhefher, D. P.: Some experiments in real data forecasting with the NCAR general circulation model. Paper presented at the national meeting of the AMS, Jan. 1969.

2. Smagorinsky, J.: Problems and promises of deterministic extended range forecasting. Wexler Memorial Lecture presented at the national meeting of the AMS, Jan. 1969.

3. Manabe, S., and Hunt, B. G.: Experiments with a stratospheric general circulation model: I. Radiative and dynamic aspects. Mon. Wea. Rev., vol. 96, no. 8, 1968.

4. Wark, D. Q., and Felming, H. E.: Indirect measurements of atmospheric temperature profiles from satellites: I. Introduction, Mon. Wea. Rev., 94, 1966.

5. Conrath, B. J.: Remote sensing of the vertical distribution of non-uniformly mixed atmospheric constituents. Proceedings of the Third Interdisciplinary Workshop on Inversion of Radiometric Measurements, J. C. Gille editor, Dept. of Meteorology, Florida State Univ., May 1968.

6. Prabhakara, C., Williamson, E. J.: Indirect determination of atmospheric ozone. Paper presented at the national meeting of the AMS, Jan. 1969.

7. House, F. B., Florance, E. T., Harrison, R., and King, J. I. F.: Meteorological inferences from radiance measurements. Final Report, under contract No. Cwb-11317, No. GCA-TR-68-18-G, GCA Corp., Bedford, Mass., Sept. 1968.

8. McKee, T. B., Whitman, R. I., and Davis, R. E.: Infrared horizon profiles for summer conditions from project Scanner. NASA TN D-4741, Washington, D. C., Aug. 1968.

9. McKee, T. B., Whitman, R. I., and Lambiotte, J. J.: A technique to infer atmospheric temperature from horizon radiance profiles. NASA TN D-5068, Washington, D. C., Aug. 1968.

10. Bates, J. C., Hanson, D. S., House, F. B., Carpenter, R. O'B., and Gille, J. C.: The synthesis of 15μ infrared horizon radiance profiles from meteorological data inputs. NASA CR-724, Washington, D. C., April 1967.

11. Gille, J. C.: On the possibility of estimating diurnal temperature variation at the stratopause from horizon radiance measurements. J. Geophys. Union, vol. 73, 1968, pp. 1863-1868.

12. Elsasser, W. M.: Atmospheric radiation tables. Meteorol. Mono., vol. 4, no. 23, Aug. 1960.

13. Anon.: Compilation of atmospheric profiles and synthesized 15μ infrared horizon radiance profiles covering the Northern Hemisphere in the longitude region between 60°W and 160°W from March 1964 through Feb. 1965. NASA-CR66184 and 66185, Washington, D. C., Oct. 1966.

14. Smith, W. L.: A polynomial representation of carbon dioxide and water vapor transmission. NESC/ESSA Tech. Report No. 47, 1969.

15. Mastenbrook, H. J.: Water vapor distribution in the stratosphere and high troposphere. J. Atmos. Sci., vol. 25, no. 2, Nov. 1968.

16. Wagner, N. K.: Theoretical accuracy of a meteorological rocketsonde thermistor. J. Appl. Meteor., vol. 3, no. 4, Aug. 1964.

NASA-Langley, 1969 —— 20 CR-1419